

1 Disruptions to the Limb Muscle Core Molecular Clock Coincide with Changes in Mitochondrial
2 Quality Control following Androgen Depletion

3

4 Michael L. Rossetti¹, Karyn A. Esser², Choogon Lee³, Robert J. Tomko Jr.³, Alexey M.
5 Eroshkin^{4,5}, Bradley S. Gordon^{1,6*}

6

7 ¹Department of Nutrition, Food and Exercise Science, Florida State University, 600 W. College
8 Avenue, Tallahassee, FL 32306

9 ²Department of Physiology and Functional Genomics, University of Florida, 1345 Center Drive,
10 PO Box 100274 Gainesville, FL 32610

11 ³Department of Biomedical Sciences, Florida State University College of Medicine, 115 W Call
12 Street, Tallahassee, FL 32304

13 ⁴Sanford Burnham Prebys Medical Discovery Institute, 10901 North Torrey Pines Road, La
14 Jolla, CA 92037

15 ⁵Rancho BioSciences, 16955 Via Del Campo #220, San Diego, CA 92127

16 ⁶Institute of Sports Sciences and Medicine, Florida State University, 600 W. Cottage Ave,
17 Tallahassee, FL 32306

18

19 Running Head: Androgens and Core Clock

20

21 *Correspondence: Bradley S. Gordon, Ph.D., Florida State University, 600 W. College Ave,

22 Tallahassee, FL 32306; Email: bsgordon@fsu.edu

23 **ABSTRACT**

24 Androgen depletion in humans leads to significant atrophy of the limb muscles.
25 However, the pathways by which androgens regulate limb muscle mass are unclear. Our
26 laboratory previously showed that mitochondrial degradation was related to the induction of
27 autophagy and the degree of muscle atrophy following androgen depletion, implying decreased
28 mitochondrial quality contributes to muscle atrophy. To increase our understanding of
29 androgen-sensitive pathways regulating decreased mitochondrial quality, total RNA from the
30 tibialis anterior of sham and castrated mice was subjected to microarray analysis. Using this
31 unbiased approach, we identified significant changes in the expression of genes that comprise the
32 core molecular clock. To assess the extent in which androgen depletion altered the limb muscle
33 clock, the tibialis anterior muscles from sham and castrated mice were harvested every 4 hr
34 throughout a diurnal cycle. The circadian expression patterns of various core clock genes and
35 known clock-controlled genes were disrupted by castration, with most genes exhibiting an
36 overall reduction in phase amplitude. Given that the core clock regulates mitochondrial quality,
37 disruption of the clock coincided with changes in the expression of genes involved with
38 mitochondrial quality control, suggesting a novel mechanism by which androgens may regulate
39 mitochondrial quality. These events coincided with an overall increase in mitochondrial
40 degradation in the muscle of castrated mice, and an increase in markers of global autophagy-
41 mediated protein breakdown. In all, these data are consistent with a novel conceptual model
42 linking androgen depletion induced limb muscle atrophy to reduced mitochondrial quality
43 control via disruption of the molecular clock.

44

45 Key Words: Testosterone, Autophagy, Muscle Atrophy

46

47 INTRODUCTION

48 Maintaining skeletal muscle mass is directly linked to a reduced risk of morbidity and
49 mortality (34, 62, 63). In males, the decrease in the production and/or bioavailability of
50 testicular androgens (termed hypogonadism) contributes to the loss of muscle mass during
51 various pathological conditions (6, 9, 21, 22, 66, 72). Though multiple muscle groups are
52 affected by hypogonadism, atrophy of the limb muscles is particularly important as they
53 comprise the large majority of total muscle mass (37), and they are the primary muscles involved
54 with physical function. Whereas limb muscle atrophy is a consequence of hypogonadism, the
55 pathways by which androgens regulate limb muscle mass remain equivocal. This is likely
56 attributed in large part to a lack of information defining the androgen-sensitive pathways in limb
57 muscles. For instance, the levator ani (LA) muscle is commonly used as a model system to study
58 androgen signaling because LA mass is highly sensitive to androgen depletion (46, 59), and use
59 of this model has shown that the canonical androgen receptor (AR) signaling pathway as a
60 predominant pathway regulating muscle mass (51, 59). Pharmacological inhibition of the
61 androgen receptor in primary myocytes and C₂C₁₂ cell culture systems yielded similar results as
62 those observed *in vivo* (5, 28). Despite the necessity of AR signaling in those models, deletion of
63 the androgen receptor did not affect mass of the limb muscles (e.g. tibialis anterior (TA)) (2, 15,
64 51, 52, 67). Rather, it was the presence of androgens themselves that dictated limb muscle mass
65 (67). This dichotomy between model systems is further illustrated by work from our laboratory
66 that showed signaling through the mechanistic target of rapamycin in complex 1 (mTORC1) was
67 dispensable for androgen-mediated growth of the limb skeletal muscles (54), even though
68 mTORC1 was absolutely required for androgen-mediated growth in AR-dependent model

69 system (1, 5), implying that androgens regulate limb muscle mass through distinct pathways that
70 have yet to be fully defined.

71 In pursuit of novel androgen-sensitive pathways in limb skeletal muscle, our laboratory
72 recently found that mitochondrial degradation was increased in the atrophied TA of mice
73 subjected to androgen depletion via castration surgery (56). Importantly, the measures of
74 degradation were related to measures of autophagy activation and the degree of muscle atrophy,
75 implying changes in mitochondrial quality control may contribute to autophagy activation and
76 subsequent limb muscle atrophy under androgen deprived conditions (56). With this idea in
77 mind, the present study subjected total RNA from the TA of those sham and castrated mice to
78 microarray analysis in order to define novel androgen-sensitive pathways in the limb skeletal
79 muscle known to regulate mitochondrial quality control. Using this unbiased approach, we
80 identified significant castration-induced changes in the expression of genes that comprise the
81 core molecular clock. The core molecular clock is a transcription-translation feedback system
82 that regulates various metabolic processes, including mitochondrial quality, by mediating diurnal
83 changes in gene expression (3, 8, 29). The positive portion of the core clock is regulated by the
84 dimer between Brain and Muscle Arntl 1 (*Bmal1*) and Circadian Locomotor Output Cycles
85 *Kaput* (*Clock*), which induce transcription of various clock-controlled genes (8). The *Period*
86 genes (*Per1-3*) and *Cryptochrome* genes (*Cry1-2*) are amongst those transcribed by the *Bmal1*-
87 *Clock* dimer (8, 58), which when translated into proteins, feedback to inhibit the transcriptional
88 activity of *BMAL1-Clock*, thus creating the negative portion of the core clock (8). Herein we
89 demonstrate that cycling and function of the core molecular clock is disrupted within the limb
90 skeletal muscle by depletion of testicular androgens, and that this disruption coincides with
91 altered expression of genes that regulate mitochondrial quality control. Alterations in

92 mitochondrial quality control overlapped with increased mitochondrial degradation (i.e.
93 mitophagy) and global autophagy activation, supporting a novel conceptual model linking
94 androgen depletion induced limb muscle atrophy to reduced mitochondrial quality control via
95 disruption of the molecular clock.

96

97 **MATERIALS and METHODS**

98 *Animals, Castration Surgery, and Experimental Design*

99 Microarray Sample Generation: The muscle samples analyzed by microarray were
100 generated from a previous study conducted by our laboratory where the objective was to
101 determine whether androgen depletion altered the molecular response following anabolic stimuli
102 (64). In brief, mice from that study were subjected to a sham or castration surgery (N = 7-8 per
103 group). Seven weeks following surgery, all mice were subjected to an overnight fast beginning
104 at 1700 hr. The next morning, sham and castrated mice were given access to food for 30 min.
105 After the refeeding, mice were fasted for an additional 4.5 hr with unrestricted access to water
106 until sacrifice occurring between 1200-1500 hr. The TA muscles were used for analysis as
107 androgens regulate mass of the TA in an AR-independent manner (67). The Institutional Animal
108 Care and Use Committee at the University of Central Florida approved these procedures and the
109 animal facility.

110 Circadian Study: Male, C57Bl/6NHsd mice (12 weeks of age) were purchased from
111 Envigo (Indianapolis, IN). Upon arrival, all mice were housed individually for 2 weeks with *ad*
112 *libitum* access to food (5001 rodent chow (LabDiet, St. Louis, MO) and water prior to being
113 randomized into 2 groups of equal body weight. One group was subjected to a castration surgery
114 to effectively stop testicular androgen production, while the other group was subjected to a sham

115 surgery in which testicular androgen production was left intact. All mice were given
116 buprenorphine (0.05 mg/kg) immediately following surgery and again 5 hr later to alleviate post-
117 operative pain. Mice recovered for 8 weeks prior to testing. Testing included sacrificing a
118 subset of mice from each group (N=3/group/time point) in alternating fashion (i.e
119 sham/castrated) every 4 hr beginning at the onset of the dark cycle (1900 hr). Food and water
120 were consumed *ad libitum* throughout the data collection. For sacrifice during the dark cycle,
121 the mouse cage was placed into a black Tupperware container under dim red light for transport to
122 a separate surgical suite. In the surgical suite, mice were lightly anesthetized with isoflurane
123 under dim red light, and then mice were euthanized via cervical dislocation. The lights were
124 then turned on and the limb muscles were rapidly extracted, and flash frozen in liquid nitrogen.
125 Preliminary tests using a HOBO light detector (Onset Computer Corp., Bourne, MA) performed
126 prior to the experiment showed that the Tupperware container prevented light exposure inside
127 the container during transport and therefore, light exposure was assumed to be negligible during
128 the actual experiment. The Animal Care and Use Committee at Florida State University
129 approved these procedures and the animal facility.

130 *RNA Extraction, Microarray and Microarray Data Analysis*

131 TA muscles (~20 mg) were homogenized in 600 μ l of Zymo Tri Reagent (Irvine, CA),
132 and RNA was isolated using a Zymo RNA Miniprep extraction kit (cat. #R2071) with on column
133 DNase treatment (Irvine, CA). RNA quantity was determined spectrophotometrically by the
134 260-to-280 nm ratio. The quality of total RNA was assessed by the Agilent Bioanalyzer Nano
135 Chip (Agilent Technologies; Santa Clara, CA), and RNA integrity scores >6 were required for
136 subsequent microarray analysis. Microarray analysis was conducted as previously described
137 (25). The microarray and microarray analysis were performed at the Sanford Burnham Prebys

138 Medical Discovery Institutes (Orlando, FL and La Jolla, CA, respectively) (N = 3/group). Lists
139 of differentially expressed genes (DEGs) were generated using a flexible *P* value (Fold Change \geq
140 1.5 and P-value without False Discovery Rate < 0.05) as this resulted in more than one hundred
141 DEGs ([Table S1](#)). A rigorous *P* value was not used for microarray analysis as it resulted in only
142 a handful of differentially expressed genes. The list of DEGs was uploaded into the publicly
143 available Database for Annotation, Visualization and Integrated Discovery (DAVID) software
144 (<https://ncifcrf.gov>) and analyzed using 2 separate algorithms: 1) Functional Category analysis,
145 and 2) KEGG Pathway analysis ([Table S2 & S3](#)). Gene expression data for this study has been
146 made available at GEO (<http://www.ncbi.nlm.nih.gov/geo>; GSE126965).

147 *cDNA Synthesis and RT-PCR*

148 cDNA was synthesized from 1.5 μ g of total RNA using a High Capacity cDNA Reverse
149 Transcription Kit (cat. #4368814; Thermo Fisher Scientific, Waltham, MA). RT-PCR was
150 conducted on either a QuantStudio3 (Thermo Fisher Scientific) or a CFX Connect (Bio-Rad,
151 Hercules, CA) RT-PCR thermal cycler using PowerUp Sybr Green Master Mix (cat. #A2742;
152 Thermo Fisher Scientific) or TaqMan Fast Advanced Master Mix (cat. #4444557; Thermo Fisher
153 Scientific). The conditions for RT-PCR with Sybr Green included an initial 2 min at 50 °C and 2
154 min at 95 °C, followed by 40 cycles which included a 15 sec denature step at 95 °C, a 15 sec
155 annealing step at 55 °C, and a 1 min extension step at 72 °C within each cycle. A melt curve
156 analysis was performed for each primer pair to ensure that a single product was efficiently
157 amplified, and the product sizes for each primer pair were verified via agarose gel
158 electrophoresis prior to experimentation. Measurement of *BNIP3* (assay ID Mm01275600_g1),
159 *Tfam* (assay ID Mm00447485_m1), *Nrf1* (assay ID Mm01135606_m1), *Parkin* (assay ID
160 Mm00450187_m1), *Pink1* (assay ID Mm00550827_m1), *Clock* (assay ID Mm00455950_m1),

161 *LC3B* (assay ID Mm00782868_sH), and *MAFbx* (assay ID Mm00499523_m1) were quantified
162 using TaqMan predesigned primer probes according to the manufacturer-recommended
163 conditions for the QuantStudio3. Relative expression levels of all genes were normalized using
164 the delta delta Ct method. *GAPDH* was used as the internal control for validation of the
165 microarray, while Ribosomal Protein Lateral Stalk Subunit P0 (*RPLP0*) was used as the internal
166 control for the circadian study as *RPLP0* expression was not affected by either time or castration
167 ([Table S4](#)). Primer sequences for all Sybr Green RT-PCR reactions are listed in Table 1. The
168 mean reaction efficiency for all experimental genes was 86.6% ± a standard deviation of 6.3%.
169 The reaction efficiencies of *RPLP0* and *GAPDH* were 87.3% and 81.3%, respectively.

170 *microRNA Analysis*

171 microRNA expression was determined using TaqMan assay primer probes (Thermo
172 Fisher Scientific) against *miR-181a* (cat. #4427975; assay ID 000480). As per the manufacturer
173 recommendations, 15 ng of total RNA (isolated using Zymo Miniprep extraction kit as described
174 above) was reverse transcribed using a miRNA Reverse Transcription kit (cat. # 4427975;
175 Thermo Fisher Scientific) with microRNA specific primers provided with each TaqMan assay.
176 Relative microRNA expression levels were normalized using the delta delta Ct method. snRNA
177 *U6* (cat. #4427975; assay ID 001973) was used as the internal control as previously
178 recommended (43). Expression of *U6* was not affected by either time or castration ([Table S4](#)).
179 Reaction efficiencies for *U6* and *miR-181a* were 95.3% and 96.8%, respectively.

180 *Western blot Analysis*

181 Western blotting was conducted as previously described with slight modifications (64).
182 Whole muscle protein from the TA was extracted by glass on glass homogenization in 10
183 volumes of buffer (10 µl/mg of muscle) consisting of 50 mM HEPES (pH 7.4), 0.1% Triton-X

184 100, 4 mM EGTA, 10 mM EDTA, 50 mM Na₄P₂O₇, 100 mM β-glycerophosphate, 25 mM NaF,
185 5 mM Na₃VO₄, and 10 μl/ml protease inhibitor cocktail (cat. #P8340, Sigma-Aldrich). Muscle
186 extract was centrifuged for 10 min at 10,000 g at 4°C, and the supernatant fraction was
187 quantified via the Bradford method. After quantification, all samples were diluted to the same
188 concentration in 2X Laemmli buffer. At each circadian time point, an equal amount of protein
189 from the 3 samples within a group (sham or castrated) was pooled together prior to Western blot
190 analysis as a way to identify potential differences between groups in diurnal protein expression
191 patterns (29). Though this method has clear limitations (i.e. inability to estimate variability at
192 each time point), this method was chosen due to limited statistical power at each time point (i.e.
193 N=3/group) and the lack of feasibility for determining relative protein expression by Western
194 blot analysis from a single cohort consisting of 36 samples. Though pooling is not the preferred
195 method for detecting differences as it can mask individual variation, others have shown that
196 pooling samples can be a viable approach to identify potential differences when experimental
197 constraints limit traditional analysis (17, 36). Thus, future work that is sufficiently powered will
198 be needed to verify differences in protein expression within each time point. Once the samples
199 were pooled, 20-60 μg of protein from each group and time point were fractionated on 4%–20%
200 Bio-Rad Tris-Glycine Criterion precast gels (Hercules, CA) and transferred to PVDF
201 membranes. Ponceau-S staining was used to assess effective transfer and equal protein loading.
202 Membranes were blocked with 5% nonfat dried milk in Tris-buffered saline + 0.1% Tween20
203 (Tris-buffered saline-Tween 20). Membranes were then incubated overnight at 4°C with
204 antibodies against BNIP3 (cat. no. 3769), Parkin (cat. no. 2132), LC3B (cat. no. 2775), p62 (cat.
205 no. 5114), COX IV (cat. no. 4844), VDAC (cat. no. 4866), Bcl-xL (cat. no. 2764), GSK3β (Ser9)
206 (cat. no. 5558), total GSK3β (cat. no. 12456), Akt (Ser473) (cat. no. 4060), total Akt (cat. no.

207 9272), and Sirt1 (cat. no. 2028), which were all obtained from Cell Signaling Technology
208 (Danvers, MA). Antibodies against Per2 were produced in house (14). Antibodies against Bmal1
209 were obtained from Sigma-Aldrich (cat. no. SAB4300614). Antibodies against 4-HNE were
210 obtained from Alpha Diagnostics (San Antonio, TX; cat. no. HNE 13-M). After incubation with
211 secondary antibodies (Bethyl Laboratories; cat. no. A120–101P or A90–116P; Sigma Aldrich;
212 cat. No. A7289), the antigen-antibody complex was visualized by enhanced chemiluminescence
213 using Clarity reagent (Bio-Rad) on a Bio-Rad ChemiDoc Touch imaging system. The exposure
214 time for all blots occurred within 10 minutes. The pixel density from all blots was quantified as
215 the ratio of total protein to the 45 kD band of the Ponceau-S stain using Image J software
216 (National Institutes of Health, Bethesda, MD) or ImageLab Software (Bio-Rad). We have
217 previously shown that our anti-mouse secondary antibody reacts non-specifically with the
218 presumed endogenous heavy chain (~50kD) and light chain (~25 kD) IgG within our mouse
219 muscle extracts (24). As such, those bands were excluded from the quantification of 4-HNE.
220 The antibodies used in this study have been previously validated by our laboratory (23, 24, 55,
221 56) or by others (7, 10, 16, 26, 60, 71, 74, 77).

222 *Cytosolic/Nuclear Fraction Separation*

223 Whole gastrocnemius muscle samples were homogenized using glass on glass in 10
224 volumes (10 μ l/mg tissue) of buffer (referred here after as buffer A) consisting of 10 mM NaCl,
225 1.5 mM MgCl₂, 20 mM HEPES, 20% glycerol, 0.1% Triton-X 100, 1 mM DTT, and 10 μ l/ml
226 protease inhibitor cocktail (Sigma Aldrich cat. #P8340, St. Louis, MO). Samples were
227 centrifuged for 5 min/2,400 $g/4^{\circ}$ C. The supernatant was collected and saved as the cytosolic
228 enriched fraction. This fraction was further centrifuged 3 times, each at 5 min/3,500 $g/4^{\circ}$ C, to
229 pellet and remove any remaining non-cytosolic material. The pellet containing the nuclear-

230 enriched fraction was then gently washed 3 times in buffer A. Between each wash, the nuclear
231 pellet was centrifuged for 5 min/2,400 g/4° C. The final nuclear pellet was then suspended in
232 400 µl of the protein extraction buffer described in the Western blot analysis section. The
233 sample was then centrifuged for 15 min/21,000 g/4° C. The supernatant was collected and saved
234 as the nuclear enriched fraction. The protein content of each fraction was quantified by the
235 Bradford method, and equal quantities of protein were diluted into 2X Laemmli buffer. At each
236 circadian time point, an equal amount of protein from each fraction generated from the 3 samples
237 within a group (sham or castrated) was pooled together prior to Western blot analysis.

238 *Statistical Analysis*

239 Circadian protein expression data from pooled samples are presented as a single value at
240 each time point. All other data are presented as mean ± SEM. Analysis of the microarray was
241 described above. Student's *t*-test was used to compare body and tissue mass between groups, and
242 to validate the microarray. Two-way ANOVA was used to assess changes in mRNA across the
243 sampling period using castration and time as the 2 factors. If an interaction was observed,
244 Fisher's LSD was used post hoc to define specific differences. Otherwise, main effects are
245 shown. Differences in protein expression patterns from ≥3 consecutive time points were initially
246 detected visually. If an expression pattern was visually observed, differences in the mean pixel
247 intensity values obtained from the ≥3 time points were assessed by Student's *t*-test. Given that
248 this study is underpowered to detect differences in protein expression at each time point, future
249 work will need to confirm the specific changes in protein expression at each time point. All
250 analysis was performed using ImageLab Software (Bio-Rad) or GraphPad Prism Software (La
251 Jolla, CA). Significance for all analysis was set at $P \leq 0.05$.

252

253 **RESULTS**

254 *Androgen depletion disrupts core clock phase and function in the limb skeletal muscle*

255 Total RNA from the TA of sham and castrated mice was analyzed by microarray.
256 DAVID bioinformatics software identified significant changes in genes that comprise
257 “Biological Rhythms” and “Circadian Rhythms” using *Functional Category* and *KEGG Pathway*
258 analyses, respectively (Tables 2 & 3). *Bmal1*, *Per2*, and *Per3* were common genes included in
259 both analyses (Table 4), and RT-PCR validation confirmed that expression of *Bmal1* was
260 decreased, and expression of *Per1-3* was increased in the atrophied TA muscle of castrated mice
261 relative to values in sham mice (Fig. 1A-D). To assess the magnitude by which androgen
262 depletion disrupted the core clock, TA muscles were harvested at 4 hr intervals across a single
263 circadian cycle from mice that were previously subjected to a sham or castration surgery. The
264 muscle and tissue characteristics of those mice are presented in Table 5 and Table 6,
265 respectively. As expected (64, 71), mass of various limb muscles was lower in the castrated
266 mice compared to the sham group without a corresponding change in tibia length or fat pad mass
267 (Table 5 & 6). The efficacy of the castration surgery was also confirmed by changes in the mass
268 of various androgen sensitive tissues, including the seminal vesicle [(55, 64) and Table 6]. Gene
269 expression of *Bmal1* and *Per1-3* in the TA of sham mice exhibited the expected circadian
270 patterns (58), and these patterns were altered in the TA of castrated mice (Fig. 1E, G-I). The
271 diurnal expression pattern of *Clock* and *Cry1* were also disrupted (Fig. 1F & J), while circadian
272 expression of *Cry2* was not different between groups (data not shown).

273 Previous work has identified various genes in skeletal muscle whose expression is under
274 the control of the core clock (45, 58), including the nuclear receptors RAR-Related Orphan
275 Receptor alpha (*RORα*) and Nuclear Receptor Subfamily 1 group D member 1 alpha (*Rev-Erba*),

276 Myogenic Differentiation (*MyoD*), D-Box Binding PAR BZIP Transcription Factor (*Dbp*), and
277 Muscle Atrophy F-Box (*MAFbx*). *Rev-Erb α* , *MyoD*, *Dbp*, and *MAFbx* each exhibited a circadian
278 expression pattern in the TA of sham mice, while *ROR α* did not (Fig. 2A-E). Androgen
279 depletion significantly altered the rhythmicity or overall expression of each gene (Fig. 2A-E),
280 suggesting androgens are required for proper core clock function in addition to the normal
281 cycling of core clock genes.

282 *Expression of various mitochondrial quality control genes are disrupted by androgen depletion*

283 The core molecular clock has been implicated in regulating the expression of genes
284 involved with mitochondrial quality control (29). Indeed, disruption of the core clock decreased
285 measures of mitochondrial function in skeletal muscle (3). This is pertinent to androgen
286 depletion as disruption of mitochondrial quality control can induce muscle atrophy (53, 61), and
287 our group previously observed a strong relationship between indices of impaired mitochondrial
288 quality and the degree of muscle atrophy following androgen depletion (56). Moreover, the
289 magnitude of change in expression of core clock genes identified by the microarray were
290 strongly related to both the indices of impaired mitochondrial quality (e.g. $r = 0.94$) and the
291 degree of muscle atrophy (e.g. $r = 0.58$) previously reported in those same samples (56).

292 Mitochondria are a dynamic organelle that change in number, size, and network
293 complexity in order to handle metabolic demand by the coordinated balance of mitochondrial
294 fission/fusion and mitochondrial biogenesis/degradation (50, 65). Mitofusion 1 & 2 (*Mfn1-2*)
295 and the Mitochondrial Dynamin Like GTPase (*Opa1*) promote fusion of mitochondria into larger
296 networks (73), while Mitochondrial fission 1 (*Fis1*) and Dynamin 1 Like (*Drp1*) promote
297 network fragmentation (73). Though genes involved with mitochondrial fission (*Drp1* and *Fis1*)
298 changed in expression over time in other tissues (29), expression of these genes did not differ by

299 time in the present study (Fig. 3A & B). However, castration lead to an overall reduction in the
300 mRNA expression of *Drp1*. Conversely, expression of genes involved with mitochondrial fusion
301 (*Opa1* and *Mfn2*) changed over time, and castration lead to an overall decrease in expression of
302 these genes (Fig. 3C & E). There was a strong trend for expression of *Mfn1* to change over time
303 ($P=0.053$) with castration causing a significant overall reduction in expression (Fig. 3D).

304 Mitochondrial biogenesis is mediated in large part by the Peroxisome Proliferator
305 Activated Receptor Gamma Co-activator 1 Alpha (PGC-1 α) signaling nexus, which regulates the
306 expression of various mitochondrial associated genes from both nuclear and mitochondrial
307 genomes (44). Expression of *PGC-1 α* is a known clock controlled gene in skeletal muscle (58),
308 and as such, *PGC-1 α* mRNA exhibited a change in expression over time (Fig. 3F). Consistent
309 with disruption of the core clock, the overall expression of *PGC-1 α* was significantly reduced in
310 the TA of castrated mice (Fig. 3F). Expression of Nuclear Respiratory Factor 1 (*Nrf1*), a co-
311 activator of PGC-1 α within the biogenesis nexus (20), was largely unaffected by castration (Fig.
312 3G). However, expression of Transcription Factor A, Mitochondrial (*Tfam*), a target gene of the
313 Nrf1-PGC-1 α transcriptional complex (33), exhibited an overall reduction (Fig. 3H), suggesting
314 impaired signaling downstream of the Nrf1-PGC-1 α complex.

315 Mitochondrial degradation is an important quality control mechanism for the removal of
316 old or dysfunctional mitochondria via the lysosomal-mediated process termed mitophagy (40),
317 which occurs through at least two distinct pathways. BCL2/Adenovirus E1B 19kDa Interacting
318 Protein 3 (BNIP3) shuttles mitochondria to the phagophore for disposal into the lysosome,
319 whereas degradation via PTEN Induced Kinase 1 (Pink1) and Parkin RBR E3 Ubiquitin Protein
320 Ligase (Parkin) involves ubiquitylation of mitochondrial proteins and subsequent shuttling to the
321 phagophore by the p62 adaptor protein (32, 49). *BNIP3* was the only mitophagy-related gene to

322 exhibit a change in expression over time, and this occurred in both groups (Fig. 3I). However,
323 castration lead to an overall reduction in the expression of *BNIP3* as well as an overall increase
324 in *Pink1* (Fig. 3I & J). Parkin mRNA was not affected by castration (Fig. 3K). In all, these data
325 suggest that genes involved with mitochondrial quality control, including those that exhibit
326 changes in expression over time, were disrupted by androgen depletion.

327 *Indices of mitophagy and autophagy activation are enhanced following androgen deprivation,*
328 *and this coincides with changes in mitochondrial protein expression patterns*

329 Mitochondrial degradation and global autophagy are enhanced when mitochondria
330 quality is impaired in order to protect the cell against adverse events such as apoptosis (12, 13,
331 47). Our previous work found that BNIP3 protein content was reduced in the TA muscle of
332 castrated mice 4 hr following consumption of a meal, but the change in BNIP3 protein did not
333 coincide with a change in the corresponding BNIP3 transcript (56). Because BNIP3 protein is
334 turned over during the mitophagy process (75), it was concluded that activation of that
335 degradative process was increased. Consistent with those previous data, the BNIP3 protein
336 expression pattern in the muscle of castrated mice exhibited an accelerated decrease from
337 circadian time 12 to 20 corresponding to the period of time when food consumption in mice is
338 elevated (Fig. 4A & H). This pattern was not matched by a change in the corresponding
339 transcript (i.e. Fig. 3I), suggesting enhanced activation of this degradative pathway. In addition
340 to BNIP3, the pattern of Parkin protein was elevated from circadian time 16 to 24 (Fig. 4B & H),
341 implying activation of this degradative pathway as well. Since Parkin-induced mitophagy occurs
342 via p62 (32), and p62 protein is degraded during this process (38), the pattern of p62 protein was
343 decreased in the muscle of castrated mice at those same time points, further supporting activation
344 of this degradative pathway (Fig. 4C & H).

345 The LC3 II/I ratio is used to represent global autophagy activation since lipidation of the
346 LC3 protein (conversion of LC3 I to LC3 II) is required for closure of the autophagosome and
347 subsequent disposal of components at the lysosome (35). Typically, a decrease in the ratio of
348 LC3 II to LC3 I suggests autophagy inhibition and vice versa (35, 38). In sham mice, the pattern
349 of the LC3 II/I ratio was lowest from circadian time 16 to 24/0 (Fig. 4D & H), consistent with
350 nutrient-mediated inhibition of this degradative process when mice consume the majority of food
351 [i.e. the dark cycle (19, 35)], and this pattern was higher from circadian time 24/0 to 8 when mice
352 are typically fasting. Interestingly, the LC3 II/I ratio pattern was lower in the muscle of castrated
353 mice from circadian time 12 to 24/0 (Fig. 4D & H), which would initially suggest greater
354 autophagy inhibition. However, comparison of the individual changes in the LC3 I and LC3 II
355 patterns suggest that LC3 I lipidation (i.e. conversion to LC3 II) and LC3 II clearance were
356 higher in the muscle of castrated mice during this time, implying enhanced autophagy activation.
357 For instance, the LC3 I pattern increased in the TA of sham mice, but not in the castrated group
358 (Fig. 4E & H), even though *LC3B* mRNA content did not differ between groups (Fig. 4G). This
359 suggests the conversion of LC3 I to II was blunted in the muscle of sham mice, but this
360 conversion was maintained in the muscle of castrated mice. Further, LC3 II is degraded when
361 autophagy is activated (35), and thus, the decrease in the LC3 II pattern that occurred only in the
362 muscle of castrated mice likely resulted from enhanced LC3 II turnover (Fig. 4F & H). The
363 notion that autophagy was increased in the muscle of castrated mice is further supported by the
364 decrease in the p62 expression pattern at these same time points (i.e. Fig. 4C), which serves as a
365 complimentary marker of autophagy activation (38). In all, these data suggest that disruption of
366 mitochondrial quality control gene expression in the limb muscle following androgen depletion

367 coincides with increased activation of BNIP3 and Pink/Parkin-mediated mitochondrial
368 degradation and global autophagy activation.

369 Markers of mitochondrial content were assessed to determine whether changes in these
370 markers coincided with the upregulation of mitochondrial degradation. Though COX IV and
371 VDAC expression appeared similar between groups at circadian time 12 to 16, the pattern of
372 COX IV was significantly lower in the muscle of castrated mice from circadian time 20 to 8 and
373 the pattern of VDAC expression was lower at circadian time 20 to 4 (Fig. 5A, B & E), coinciding
374 with the observed increase in markers of mitophagy pathway activation (i.e. Fig. 4). The Bcl-xl
375 expression pattern was also lower in the muscle of castrated mice from circadian time 12 to 20
376 before returning to sham values for the remainder of the time course (Fig. 5C & E), suggesting a
377 compensatory effect by the muscle to maintain levels of this antiapoptotic protein (30). The
378 pattern of 4-HNE, a free radical byproduct, was higher in the muscle of castrated mice prior to
379 the change in the mitochondrial protein expression pattern, and this elevation persisted
380 throughout the remaining sampling time course (Fig. 5D & E), suggesting production of reactive
381 oxygen species coincided with enhanced turnover of mitochondrial proteins following androgen
382 depletion.

383 *Various regulators of the core clock are altered in the limb muscle following androgen depletion*

384 The most evident change to the core clock following androgen depletion was an overall
385 reduction in the phase amplitude of clock-controlled genes. In addition to regulating *Bmal1* gene
386 transcription, MyoD also feeds back to enhance the transcriptional activity of the Bmal1-Clock
387 dimer in skeletal muscle (27). As such, the reduction in *MyoD* (i.e. Fig. 2) may have contributed
388 to impaired transcription of Bmal1-Clock target genes (i.e. *Dbp*). Despite reduced amplitude of
389 Bmal1-Clock target genes, we observed a contradictory increase in the protein expression pattern

390 of Bmal1 in the muscle of castrated mice from circadian time 24/0 to 8 (Fig. 6A & E). Further
391 analysis indicates that impairment of Bmal1-Clock transcription was not due to Bmal1 protein
392 export from the nucleus as Bmal1 protein content appeared to be higher in the nuclear-enriched
393 fraction from gastrocnemius muscles of castrated mice from circadian time 24/0 to 8, (long
394 exposure Fig. 6B).

395 Previous work found that loss of Glycogen Synthase Kinase 3 β (GSK3 β) function not
396 only impaired Bmal1-Clock transcriptional activity, but it resulted in accumulation of Bmal1
397 protein (57). Accordingly, the pattern of GSK3 β phosphorylation on the inhibitory Ser9 site
398 was higher in the muscle of castrated mice at the circadian times where the Bmal1 protein pattern
399 was also elevated (Fig. 6C & E), suggesting inhibition of GSK3 β function may have contributed
400 in part to disruption of the muscle clock and the observed increase in Bmal1 protein expression
401 pattern. Akt phosphorylates GSK3 β on Ser9 to inhibit function (11), and we previously found
402 Akt phosphorylation to be increased in the muscle following androgen deprivation (55, 56).
403 Though phosphorylation pattern of Akt (Thr308) did not appear different between groups (Data
404 not shown), the phosphorylation pattern of Akt (Ser473) was higher in the muscle of castrated
405 mice from circadian times 24/0 to 8 (Fig. 6D & E), implying activation of Akt may have also
406 contributed to disruption of the clock via GSK3 β .

407 The Per2-Cry dimer also represses Bmal1-Clock transcriptional activity (8), with changes
408 in expression of Per2 being the primary factor mediating this repression (10). Consistent with
409 reduced amplitude of Bmal1-Clock target genes, the pattern of total Per2 protein was higher in
410 the TA of castrated mice from circadian time 20 to 4 (Fig. 7A & F). Per2 undergoes extensive
411 phosphorylation as a signal to induce degradation (41, 69), and changes in Per2 phosphorylation
412 can be observed by altered migration by SDS-PAGE (41). Consequently, the pattern of Per2 in

413 the faster migrating immunoreactive band was higher in the muscle of castrated mice (lower
414 band Fig. 7B & F), indicating accumulation of Per2 was due at least in part to reduced
415 phosphorylation.

416 Sirtuin 1 (Sirt1) is an NAD(+)-dependent deacetylase whose protein not only exhibits a
417 circadian expression pattern, but also regulates function of the core clock genes by promoting
418 degradation of the Per2 protein (4). Sirt1 protein exhibited the anticipated circadian expression
419 pattern in the TA of sham mice (Fig. 7C & F), but, this pattern was completely lost in the muscle
420 of castrated mice (Fig. 7C & F) as the overall pattern was lower throughout the sampling period.
421 Interestingly, this overall reduction in the Sirt1 protein pattern was independent of changes in the
422 corresponding *Sirt1* transcript (Fig. 7D), implying post transcriptional regulation of the Sirt1
423 protein.

424 MicroRNA 181a (*miR-181a*) not only influenced core clock function in other tissues
425 (39), but it also repressed Sirt1 expression at the level of translation (76), implying a potential
426 role for change in this microRNA in the regulation of Sirt1. *miR-181a* expression oscillated in
427 the muscle of both groups across the sampling period (main effect of time), but *miR-181a* levels
428 were significantly higher in the TA of castrated mice at circadian time 24/0 (Fig. 7E),
429 corresponding to the circadian time where Sirt1 protein expression pattern peaked in sham mice
430 (i.e. Fig. 7C). While this implies a potential repressive role for *miR-181a* at that time point, other
431 factors likely contributed to the overall reduction in the Sirt1 protein pattern at other time points.
432 In all, these data suggest that disruption of the clock following androgen deprivation is likely due
433 to changes to various known clock regulatory components.

434

435 **DISCUSSION**

436 The absence of circulating androgens contributes to atrophy of the limb skeletal muscles
437 (21, 22, 68), however, the underlying mechanisms remain ill-defined. For instance, the
438 canonical AR signaling pathway is not required for maintenance of limb skeletal muscle mass (2,
439 15, 51, 67). Previous work by our laboratory provided initial evidence that altered mitochondrial
440 quality may contribute to limb muscle atrophy as mitochondrial degradation was related to the
441 induction of autophagy markers and the degree of muscle atrophy (56). During our search for
442 regulatory mechanisms that mediate mitochondrial quality, we identified changes in genes
443 associated with the core clock (e.g. *Bmal1*). Since the core clock regulates mitochondrial quality
444 in skeletal muscle (3) and other tissues [i.e. liver (29)], we hypothesized that disruption to the
445 core clock may coincide with impaired mitochondrial quality control following androgen
446 depletion. Consequently, our current findings show that disruption of the core clock following
447 androgen depletion coincides with altered expression of various genes involved with
448 mitochondrial quality control, including those that exhibit a change in expression over time.
449 This disruption overlapped with indices of enhanced mitochondrial degradation (mitophagy),
450 global autophagy activation, and subsequent muscle atrophy. Therefore, we posit a novel
451 conceptual model linking androgen depletion-induced limb muscle atrophy to reduced
452 mitochondrial quality control via disruption of the molecular clock (Fig. 8).

453 The results of the present study provide evidence that atrophy of the limb muscle
454 following androgen depletion may be due in part to changes in core clock-mediated regulation of
455 mitochondrial quality control. Despite this notion, disrupting the core clock in adult skeletal
456 muscle via inducible deletion of *Bmal1* was not sufficient to induce atrophy in previous work
457 (18, 58), questioning this as a mechanism in the regulation of limb muscle mass. One possible
458 explanation is that only some mitochondrial quality control genes exhibited a change in

459 expression over time, implying that disruption of the core clock contributes to, but is not the only
460 cause of, decreased mitochondrial quality control following androgen depletion. Indeed, analysis
461 of publicly available gene arrays from the gastrocnemius of adult mice in which the muscle clock
462 was disrupted via inducible *Bmal1* deletion (58) showed that *Pink1*, which did not exhibit
463 changes in expression over time in our study, was unaffected by deletion of *Bmal1*. Conversely,
464 *PGC-1 α* and *BNIP3*, which did exhibit changes in expression over time in our study, were
465 altered by deleting *Bmal1*. This suggests that the *Bmal1*-Clock transcriptional dimer is
466 responsible for expression of some, but not all mitochondrial quality control genes. An
467 alternative explanation is that disruption of *Bmal1*-Clock in combination with changes in other
468 core clock regulatory factors may contribute to the regulation of mitochondrial quality control
469 and subsequent muscle mass. For instance, maintaining *Sirt1* protein expression following
470 nutrient deprivation preserved muscle mass by inhibiting the transcription of genes involved with
471 muscle protein breakdown including *MAFbx* and *BNIP3* (42). That mechanism of *Sirt1* action
472 with fasting would not be consistent with findings in the present study as *MAFbx* and *BNIP3*
473 mRNA were suppressed in the muscle under androgen-deprived conditions (i.e. Fig. 2 & 3 and
474 (31, 56)), suggesting an alternative mechanism. A more likely explanation is the decrease in
475 muscle mass was due to the failure of *Sirt1* to mediate degradation of *Per2*, which would disrupt
476 not only the *Bmal1*-Clock transcriptional activity, but possibly expression of other genes that
477 regulate muscle mass as well. For instance, in addition to mediating *Bmal1*-Clock function, *Per2*
478 has also been shown to regulate expression of mitochondrial genes (48) and to regulate growth in
479 ovarian tumors (70). Therefore, the way in which the clock is disrupted under androgen-
480 deprived conditions (i.e. decreased *Sirt1* and increased *Per2*) may have a different effect on
481 muscle mass compared to inhibition of just the *Bmal1*-Clock transcriptional complex.

482 It is known that testosterone is released in a circadian manner, but the sensitivity of the
483 limb muscle clock to changes in testosterone concentration remains unknown. Our group
484 showed that castration decreased plasma testosterone in mice by ~70% (56, 64), which is
485 sufficient to disrupt the clock (Fig. 1 & 2). A previous study from our laboratory showed that
486 administering Nandrolone Decanoate (ND) to previously castrated mice restored muscle mass
487 (54). In that study, the TA muscles were harvested 7 days following the final ND injection.
488 Even though muscle mass was completely restored by ND administration (54), testosterone
489 levels at the time of sacrifice were reduced by ~50% compared to sham values (Data not shown).
490 While that study was not properly designed to analyze changes to the core clock, the expression
491 of some core clock genes (e.g. *Per1* and *Per3*) were restored to sham levels by ND
492 administration while others (e.g. *Clock* and *ROR α*) were not (Data not shown). This suggests
493 that the sensitivity of the core clock to changes in circulating testosterone may be gene
494 dependent, and will require additional work to assess the sensitivity of the core clock to changes
495 in circulating testosterone.

496 In humans, androgens have been deemed to regulate muscle mass in large part by
497 blunting muscle protein breakdown during the fasted metabolic state (21, 22). In contrast, our
498 data show that markers of autophagy, oxidative stress, and mitochondrial degradation (e.g.
499 increased Parkin and BNIP3 protein content, decreased p62 protein content) were increased in
500 the muscle of castrated mice during a time when these nocturnal animals consume much of their
501 food (i.e. circadian time 12-24). Given that we previously showed a strong relationship between
502 mitochondrial degradation and autophagy activation (56), it is possible that nutrient consumption
503 initiates mitochondrial stress, leading to the subsequent increase in autophagy-mediated protein
504 breakdown that persists into the post-absorptive state (12, 13). This idea is supported by our

505 recent finding in that markers of mitophagy were increased in the muscle of castrated mice that
506 were refed following an overnight fast (56), but those same markers of mitophagy were not
507 altered if castrated mice remained fasted despite elevated markers of autophagy [(64) and
508 unpublished observations]. Future work is needed to understand whether increased availability
509 of ATP producing substrates (i.e. fatty acids and/or NADH+) might impose a detrimental stress
510 on the mitochondria in the limb muscle under androgen-deprived conditions, and whether this
511 effect is augmented by disruption of the core clock.

512 In conclusion, we provide evidence that androgen depletion disrupts the core molecular
513 clock in the limb skeletal muscle, and this disruption coincides with changes in mitochondrial
514 quality control and subsequent muscle atrophy. The change in expression of mitochondrial
515 quality control genes coincides with an increase in mitochondrial degradation pathway activation
516 and subsequent change to the circadian expression pattern of mitochondrial proteins. As
517 mitochondrial health is an emerging and important regulator of skeletal muscle mass, these data
518 support a novel conceptual model linking androgen depletion-induced limb muscle atrophy to
519 reduced mitochondrial quality control via disruption of the molecular clock. Such knowledge
520 will be useful for developing therapies that treat limb muscle atrophy in hypogonadal males that
521 are unable to receive androgen replacement therapy.

522

523 **ACKNOWLEDGMENTS**

524 The authors would like to thank Dr. Jennifer Steiner for critical discussion and review of the
525 manuscript.

526

527 **GRANTS**

528 This project was supported through funds provided by the University of Central Florida and the
529 Institute for Successful Longevity (BSG), NIH grants R01AR066082 (KAE) and NS-099813
530 (CL).

531

532 **DISCLOSURES**

533 The authors have no disclosures.

534

535 **REFERENCES**

- 536 1. **Altamirano F, Oyarce C, Silva P, Toyos M, Wilson C, Lavandero S, Uhlén P, and**
537 **Estrada M.** Testosterone induces cardiomyocyte hypertrophy through mammalian target of
538 rapamycin complex 1 pathway. *J Endocrinol* 202: 299-307, 2009.
- 539 2. **Altuwaijri S, Lee DK, Chuang KH, Ting HJ, Yang Z, Xu Q, Tsai MY, Yeh S,**
540 **Hanchett LA, Chang HC, and Chang C.** Androgen receptor regulates expression of skeletal
541 muscle-specific proteins and muscle cell types. *Endocrine* 25: 27-32, 2004.
- 542 3. **Andrews JL, Zhang X, McCarthy JJ, McDearmon EL, Hornberger TA, Russell B,**
543 **Campbell KS, Arbogast S, Reid MB, Walker JR, Hogenesch JB, Takahashi JS, and Esser**
544 **KA.** CLOCK and BMAL1 regulate MyoD and are necessary for maintenance of skeletal muscle
545 phenotype and function. *Proc Natl Acad Sci U S A* 107: 19090-19095, 2010.
- 546 4. **Asher G, Gatfield D, Stratmann M, Reinke H, Dibner C, Kreppel F, Mostoslavsky**
547 **R, Alt FW, and Schibler U.** SIRT1 regulates circadian clock gene expression through PER2
548 deacetylation. *Cell* 134: 317-328, 2008.

- 549 5. **Basualto-Alarcón C, Jorquera G, Altamirano F, Jaimovich E, and Estrada M.**
550 Testosterone signals through mTOR and androgen receptor to induce muscle hypertrophy. *Med*
551 *Sci Sports Exerc* 45: 1712-1720, 2013.
- 552 6. **Bhasin S, Storer TW, Berman N, Yarasheski KE, Clevenger B, Phillips J, Lee WP,**
553 **Bunnell TJ, and Casaburi R.** Testosterone replacement increases fat-free mass and muscle size
554 in hypogonadal men. *J Clin Endocrinol Metab* 82: 407-413, 1997.
- 555 7. **Brown JL, Rosa-Caldwell ME, Lee DE, Blackwell TA, Brown LA, Perry RA,**
556 **Haynie WS, Hardee JP, Carson JA, Wiggs MP, Washington TA, and Greene NP.**
557 Mitochondrial degeneration precedes the development of muscle atrophy in progression of
558 cancer cachexia in tumour-bearing mice. *J Cachexia Sarcopenia Muscle* 2017.
- 559 8. **Buhr ED, and Takahashi JS.** Molecular components of the Mammalian circadian clock.
560 *Handb Exp Pharmacol* 3-27, 2013.
- 561 9. **Burney BO, and Garcia JM.** Hypogonadism in male cancer patients. *J Cachexia*
562 *Sarcopenia Muscle* 3: 149-155, 2012.
- 563 10. **Chen R, Schirmer A, Lee Y, Lee H, Kumar V, Yoo SH, Takahashi JS, and Lee C.**
564 Rhythmic PER abundance defines a critical nodal point for negative feedback within the
565 circadian clock mechanism. *Mol Cell* 36: 417-430, 2009.
- 566 11. **Cross DA, Alessi DR, Cohen P, Andjelkovich M, and Hemmings BA.** Inhibition of
567 glycogen synthase kinase-3 by insulin mediated by protein kinase B. *Nature* 378: 785-789, 1995.
- 568 12. **Cárdenas C, Miller RA, Smith I, Bui T, Molgó J, Müller M, Vais H, Cheung KH,**
569 **Yang J, Parker I, Thompson CB, Birnbaum MJ, Hallows KR, and Foscett JK.** Essential
570 regulation of cell bioenergetics by constitutive InsP3 receptor Ca²⁺ transfer to mitochondria.
571 *Cell* 142: 270-283, 2010.

- 572 13. **Cárdenas C, Müller M, McNeal A, Lovy A, Jaña F, Bustos G, Urra F, Smith N,**
573 **Molgó J, Diehl JA, Ridky TW, and Foskett JK.** Selective Vulnerability of Cancer Cells by
574 Inhibition of Ca(2+) Transfer from Endoplasmic Reticulum to Mitochondria. *Cell Rep* 15: 219-
575 220, 2016.
- 576 14. **D'Alessandro M, Beesley S, Kim JK, Jones Z, Chen R, Wi J, Kyle K, Vera D,**
577 **Pagano M, Nowakowski R, and Lee C.** Stability of Wake-Sleep Cycles Requires Robust
578 Degradation of the PERIOD Protein. *Curr Biol* 27: 3454-3467.e3458, 2017.
- 579 15. **De Gendt K, and Verhoeven G.** Tissue- and cell-specific functions of the androgen
580 receptor revealed through conditional knockout models in mice. *Mol Cell Endocrinol* 352: 13-25,
581 2012.
- 582 16. **Dennis MD, Coleman CS, Berg A, Jefferson LS, and Kimball SR.** REDD1 enhances
583 protein phosphatase 2A-mediated dephosphorylation of Akt to repress mTORC1 signaling. *Sci*
584 *Signal* 7: ra68, 2014.
- 585 17. **Diz AP, Truebano M, and Skibinski DO.** The consequences of sample pooling in
586 proteomics: an empirical study. *Electrophoresis* 30: 2967-2975, 2009.
- 587 18. **Dyar KA, Hubert MJ, Mir AA, Ciciliot S, Lutter D, Greulich F, Quagliarini F,**
588 **Kleinert M, Fischer K, Eichmann TO, Wright LE, Peña Paz MI, Casarin A, Pertegato V,**
589 **Romanello V, Albiero M, Mazzucco S, Rizzuto R, Salviati L, Biolo G, Blaauw B, Schiaffino**
590 **S, and Uhlénhaut NH.** Transcriptional programming of lipid and amino acid metabolism by the
591 skeletal muscle circadian clock. *PLoS Biol* 16: e2005886, 2018.
- 592 19. **Ellacott KL, Morton GJ, Woods SC, Tso P, and Schwartz MW.** Assessment of
593 feeding behavior in laboratory mice. *Cell Metab* 12: 10-17, 2010.

- 594 20. **Fernandez-Marcos PJ, and Auwerx J.** Regulation of PGC-1 α , a nodal regulator of
595 mitochondrial biogenesis. *Am J Clin Nutr* 93: 884S-890, 2011.
- 596 21. **Ferrando AA, Sheffield-Moore M, Paddon-Jones D, Wolfe RR, and Urban RJ.**
597 Differential anabolic effects of testosterone and amino acid feeding in older men. *J Clin*
598 *Endocrinol Metab* 88: 358-362, 2003.
- 599 22. **Ferrando AA, Sheffield-Moore M, Yeckel CW, Gilkison C, Jiang J, Achacosa A,**
600 **Lieberman SA, Tipton K, Wolfe RR, and Urban RJ.** Testosterone administration to older men
601 improves muscle function: molecular and physiological mechanisms. *Am J Physiol Endocrinol*
602 *Metab* 282: E601-607, 2002.
- 603 23. **Gordon BS, Delgado-Diaz DC, Carson J, Fayad R, Wilson LB, and Kostek MC.**
604 Resveratrol improves muscle function but not oxidative capacity in young mdx mice. *Can J*
605 *Physiol Pharmacol* 92: 243-251, 2014.
- 606 24. **Gordon BS, Liu C, Steiner JL, Nader GA, Jefferson LS, and Kimball SR.** Loss of
607 REDD1 augments the rate of the overload-induced increase in muscle mass. *Am J Physiol Regul*
608 *Integr Comp Physiol* 311: R545-557, 2016.
- 609 25. **Gordon BS, Steiner JL, Rossetti ML, Qiao S, Ellisen LW, Govindarajan SS,**
610 **Eroshkin AM, Williamson DL, and Coen PM.** REDD1 induction regulates the skeletal muscle
611 gene expression signature following acute aerobic exercise. *Am J Physiol Endocrinol Metab* 313:
612 E737-E747, 2017.
- 613 26. **Hodge BA, Wen Y, Riley LA, Zhang X, England JH, Harfmann BD, Schroder EA,**
614 **and Esser KA.** The endogenous molecular clock orchestrates the temporal separation of
615 substrate metabolism in skeletal muscle. *Skelet Muscle* 5: 17, 2015.

- 616 27. **Hodge BA, Zhang X, Gutierrez-Monreal MA, Cao Y, Hammers DW, Yao Z, Wolff**
617 **CA, Du P, Kemler D, Judge AR, and Esser KA.** MYOD1 functions as a clock amplifier as
618 well as a critical co-factor for downstream circadian gene expression in muscle. *Elife* 8: 2019.
- 619 28. **Hughes DC, Stewart CE, Sculthorpe N, Dugdale HF, Yousefian F, Lewis MP, and**
620 **Sharples AP.** Testosterone enables growth and hypertrophy in fusion impaired myoblasts that
621 display myotube atrophy: deciphering the role of androgen and IGF-I receptors. *Biogerontology*
622 17: 619-639, 2016.
- 623 29. **Jacobi D, Liu S, Burkewitz K, Kory N, Knudsen NH, Alexander RK, Unluturk U, Li**
624 **X, Kong X, Hyde AL, Gangl MR, Mair WB, and Lee CH.** Hepatic Bmal1 Regulates
625 Rhythmic Mitochondrial Dynamics and Promotes Metabolic Fitness. *Cell Metab* 22: 709-720,
626 2015.
- 627 30. **Janumyan YM, Sansam CG, Chattopadhyay A, Cheng N, Soucie EL, Penn LZ,**
628 **Andrews D, Knudson CM, and Yang E.** Bcl-xL/Bcl-2 coordinately regulates apoptosis, cell
629 cycle arrest and cell cycle entry. *EMBO J* 22: 5459-5470, 2003.
- 630 31. **Jiao Q, Pruznak AM, Huber D, Vary TC, and Lang CH.** Castration differentially
631 alters basal and leucine-stimulated tissue protein synthesis in skeletal muscle and adipose tissue.
632 *Am J Physiol Endocrinol Metab* 297: E1222-1232, 2009.
- 633 32. **Jin SM, and Youle RJ.** PINK1- and Parkin-mediated mitophagy at a glance. *J Cell Sci*
634 125: 795-799, 2012.
- 635 33. **Jornayvaz FR, and Shulman GI.** Regulation of mitochondrial biogenesis. *Essays*
636 *Biochem* 47: 69-84, 2010.

- 637 34. **Joskova V, Patkova A, Havel E, Najpaverova S, Uramova D, Kovarik M, Zadak Z,**
638 **and Hronek M.** Critical evaluation of muscle mass loss as a prognostic marker of morbidity in
639 critically ill patients and methods for its determination. *J Rehabil Med* 50: 696-704, 2018.
- 640 35. **Ju JS, Varadhachary AS, Miller SE, and Weihl CC.** Quantitation of "autophagic flux"
641 in mature skeletal muscle. *Autophagy* 6: 929-935, 2010.
- 642 36. **Kendzioriski C, Irizarry RA, Chen KS, Haag JD, and Gould MN.** On the utility of
643 pooling biological samples in microarray experiments. *Proc Natl Acad Sci U S A* 102: 4252-
644 4257, 2005.
- 645 37. **Kim J, Wang Z, Heymsfield SB, Baumgartner RN, and Gallagher D.** Total-body
646 skeletal muscle mass: estimation by a new dual-energy X-ray absorptiometry method. *Am J Clin*
647 *Nutr* 76: 378-383, 2002.
- 648 38. **Klionsky DJ, Abdelmohsen K, Abe A, Abedin MJ, Abeliovich H, Acevedo Arozena**
649 **A, Adachi H, Adams CM, Adams PD, Adeli K, Adhietty PJ, Adler SG, Agam G, Agarwal**
650 **R, Aghi MK, Agnello M, Agostinis P, Aguilar PV, Aguirre-Ghiso J, Airoidi EM, Ait-Si-Ali**
651 **S, Akematsu T, Akporiaye ET, Al-Rubeai M, Albaiceta GM, Albanese C, Albani D, Albert**
652 **ML, Aldudo J, Algül H, Alirezaei M, Alloza I, Almasan A, Almonte-Beceril M, Alnemri ES,**
653 **Alonso C, Altan-Bonnet N, Altieri DC, Alvarez S, Alvarez-Erviti L, Alves S, Amadoro G,**
654 **Amano A, Amantini C, Ambrosio S, Amelio I, Amer AO, Amessou M, Amon A, An Z,**
655 **Anania FA, Andersen SU, Andley UP, Andreadi CK, Andrieu-Abadie N, Anel A, Ann DK,**
656 **Anoopkumar-Dukie S, Antonioli M, Aoki H, Apostolova N, Aquila S, Aquilano K, Araki K,**
657 **Arama E, Aranda A, Araya J, Arcaro A, Arias E, Arimoto H, Ariosa AR, Armstrong JL,**
658 **Arnould T, Arsov I, Asanuma K, Askanas V, Asselin E, Atarashi R, Atherton SS, Atkin JD,**
659 **Attardi LD, Auberger P, Auburger G, Aurelian L, Autelli R, Avagliano L, Avantaggiati**

660 ML, Avrahami L, Awale S, Azad N, Bachetti T, Backer JM, Bae DH, Bae JS, Bae ON, Bae
661 SH, Baehrecke EH, Baek SH, Baghdiguian S, Bagniewska-Zadworna A, Bai H, Bai J, Bai
662 XY, Bailly Y, Balaji KN, Balduini W, Ballabio A, Balzan R, Banerjee R, Bánhegyi G, Bao
663 H, Barbeau B, Barrachina MD, Barreiro E, Bartel B, Bartolomé A, Bassham DC, Bassi
664 MT, Bast RC, Basu A, Batista MT, Batoko H, Battino M, Bauckman K, Baumgarner BL,
665 Bayer KU, Beale R, Beaulieu JF, Beck GR, Becker C, Beckham JD, Bédard PA, Bednarski
666 PJ, Begley TJ, Behl C, Behrends C, Behrens GM, Behrns KE, Bejarano E, Belaid A,
667 Belleudi F, Bénard G, Berchem G, Bergamaschi D, Bergami M, Berkhout B, Berliocchi L,
668 Bernard A, Bernard M, Bernassola F, Bertolotti A, Bess AS, Besteiro S, Bettuzzi S, Bhalla
669 S, Bhattacharyya S, Bhutia SK, Biagosch C, Bianchi MW, Biard-Piechaczyk M, Billes V,
670 Bincoletto C, Bingol B, Bird SW, Bitoun M, Bjedov I, Blackstone C, Blanc L, Blanco GA,
671 Blomhoff HK, Boada-Romero E, Böckler S, Boes M, Boesze-Battaglia K, Boise LH, Bolino
672 A, Boman A, Bonaldo P, Bordi M, Bosch J, Botana LM, Botti J, Bou G, Bouché M,
673 Bouchecareilh M, Boucher MJ, Boulton ME, Bouret SG, Boya P, Boyer-Guittaut M,
674 Bozhkov PV, Brady N, Braga VM, Brancolini C, Braus GH, Bravo-San Pedro JM,
675 Brennan LA, Bresnick EH, Brest P, Bridges D, Bringer MA, Brini M, Brito GC, Brodin B,
676 Brookes PS, Brown EJ, Brown K, Broxmeyer HE, Bruhat A, Brum PC, Brumell JH,
677 Brunetti-Pierri N, Bryson-Richardson RJ, Buch S, Buchan AM, Budak H, Bulavin DV,
678 Bultman SJ, Bultynck G, Bumbasirevic V, Burelle Y, Burke RE, Burmeister M, Bütikofer
679 P, Caberlotto L, Cadwell K, Cahova M, Cai D, Cai J, Cai Q, Calatayud S, Camougrand N,
680 Campanella M, Campbell GR, Campbell M, Campello S, Candau R, Caniggia I, Cantoni
681 L, Cao L, Caplan AB, Caraglia M, Cardinali C, Cardoso SM, Carew JS, Carleton LA,
682 Carlin CR, Carloni S, Carlsson SR, Carmona-Gutierrez D, Carneiro LA, Carnevali O,

683 Carra S, Carrier A, Carroll B, Casas C, Casas J, Cassinelli G, Castets P, Castro-Obregon
684 S, Cavallini G, Ceccherini I, Cecconi F, Cederbaum AI, Ceña V, Cenci S, Cerella C, Cervia
685 D, Cetrullo S, Chaachouay H, Chae HJ, Chagin AS, Chai CY, Chakrabarti G, Chamilos G,
686 Chan EY, Chan MT, Chandra D, Chandra P, Chang CP, Chang RC, Chang TY, Chatham
687 JC, Chatterjee S, Chauhan S, Che Y, Cheetham ME, Cheluvappa R, Chen CJ, Chen G,
688 Chen GC, Chen H, Chen JW, Chen JK, Chen M, Chen P, Chen Q, Chen SD, Chen S, Chen
689 SS, Chen W, Chen WJ, Chen WQ, Chen X, Chen YH, Chen YG, Chen Y, Chen YJ, Chen
690 YQ, Chen Z, Cheng A, Cheng CH, Cheng H, Cheong H, Cherry S, Chesney J, Cheung CH,
691 Chevet E, Chi HC, Chi SG, Chiacchiera F, Chiang HL, Chiarelli R, Chiariello M, Chieppa
692 M, Chin LS, Chiong M, Chiu GN, Cho DH, Cho SG, Cho WC, Cho YY, Cho YS, Choi AM,
693 Choi EJ, Choi EK, Choi J, Choi ME, Choi SI, Chou TF, Chouaib S, Choubey D, Choubey
694 V, Chow KC, Chowdhury K, Chu CT, Chuang TH, Chun T, Chung H, Chung T, Chung
695 YL, Chwae YJ, Cianfanelli V, Ciarcia R, Ciechomska IA, Ciriolo MR, Cirone M,
696 Claerhout S, Clague MJ, Clària J, Clarke PG, Clarke R, Clementi E, Cleyrat C, Cnop M,
697 Coccia EM, Cocco T, Codogno P, Coers J, Cohen EE, Colecchia D, Coletto L, Coll NS,
698 Colucci-Guyon E, Comincini S, Condello M, Cook KL, Coombs GH, Cooper CD, Cooper
699 JM, Coppens I, Corasaniti MT, Corazzari M, Corbalan R, Corcelle-Termeau E, Cordero
700 MD, Corral-Ramos C, Corti O, Cossarizza A, Costelli P, Costes S, Cotman SL, Coto-
701 Montes A, Cottet S, Couve E, Covey LR, Cowart LA, Cox JS, Coxon FP, Coyne CB, Cragg
702 MS, Craven RJ, Crepaldi T, Crespo JL, Criollo A, Crippa V, Cruz MT, Cuervo AM,
703 Cuezva JM, Cui T, Cutillas PR, Czaja MJ, Czyzyk-Krzeska MF, Dagda RK, Dahmen U,
704 Dai C, Dai W, Dai Y, Dalby KN, Dalla Valle L, Dalmaso G, D'Amelio M, Damme M,
705 Darfeuille-Michaud A, Dargemont C, Darley-USmar VM, Dasarathy S, Dasgupta B, Dash

706 S, Dass CR, Davey HM, Davids LM, Dávila D, Davis RJ, Dawson TM, Dawson VL, Daza P,
707 de Belleruche J, de Figueiredo P, de Figueiredo RC, de la Fuente J, De Martino L, De
708 Matteis A, De Meyer GR, De Milito A, De Santi M, de Souza W, De Tata V, De Zio D,
709 Debnath J, Dechant R, Decuypere JP, Deegan S, Dehay B, Del Bello B, Del Re DP, Delage-
710 Mourroux R, Delbridge LM, Deldicque L, Delorme-Axford E, Deng Y, Dengjel J, Denizot
711 M, Dent P, Der CJ, Deretic V, Derrien B, Deutsch E, Devarenne TP, Devenish RJ, Di
712 Bartolomeo S, Di Daniele N, Di Domenico F, Di Nardo A, Di Paola S, Di Pietro A, Di Renzo
713 L, DiAntonio A, Díaz-Araya G, Díaz-Laviada I, Diaz-Meco MT, Diaz-Nido J, Dickey CA,
714 Dickson RC, Diederich M, Digard P, Dikic I, Dinesh-Kumar SP, Ding C, Ding WX, Ding Z,
715 Dini L, Distler JH, Diwan A, Djavaheri-Mergny M, Dmytruk K, Dobson RC, Doetsch V,
716 Dokladny K, Dokudovskaya S, Donadelli M, Dong XC, Dong X, Dong Z, Donohue TM,
717 Doran KS, D'Orazi G, Dorn GW, Dosenko V, Dridi S, Drucker L, Du J, Du LL, Du L, du
718 Toit A, Dua P, Duan L, Duann P, Dubey VK, Duchen MR, Duchosal MA, Duez H, Dugail I,
719 Dumit VI, Duncan MC, Dunlop EA, Dunn WA, Dupont N, Dupuis L, Durán RV, Durcan
720 TM, Duvezin-Caubet S, Duvvuri U, Eapen V, Ebrahimi-Fakhari D, Echard A, Eckhart L,
721 Edelstein CL, Edinger AL, Eichinger L, Eisenberg T, Eisenberg-Lerner A, Eissa NT, El-
722 Deiry WS, El-Khoury V, Elazar Z, Eldar-Finkelman H, Elliott CJ, Emanuele E,
723 Emmenegger U, Engedal N, Engelbrecht AM, Engelender S, Enserink JM, Erdmann R,
724 Erenpreisa J, Eri R, Eriksen JL, Erman A, Escalante R, Eskelinen EL, Espert L, Esteban-
725 Martínez L, Evans TJ, Fabri M, Fabrias G, Fabrizi C, Facchiano A, Færgeman NJ,
726 Faggioni A, Fairlie WD, Fan C, Fan D, Fan J, Fang S, Fanto M, Fanzani A, Farkas T,
727 Faure M, Favier FB, Fearnhead H, Federici M, Fei E, Felizardo TC, Feng H, Feng Y,
728 Ferguson TA, Fernández Á, Fernandez-Barrena MG, Fernandez-Checa JC, Fernández-

729 **López A, Fernandez-Zapico ME, Feron O, Ferraro E, Ferreira-Halder CV, Fesus L, Feuer**
730 **R, Fiesel FC, Filippi-Chiela EC, Filomeni G, Fimia GM, Fingert JH, Finkbeiner S, Finkel**
731 **T, Fiorito F, Fisher PB, Flajolet M, Flamigni F, Florey O, Florio S, Floto RA, Folini M,**
732 **Follo C, Fon EA, Fornai F, Fortunato F, Fraldi A, Franco R, Francois A, François A,**
733 **Frankel LB, Fraser ID, Frey N, Freyssenet DG, Frezza C, Friedman SL, Frigo DE, Fu D,**
734 **Fuentes JM, Fueyo J, Fujitani Y, Fujiwara Y, Fujiya M, Fukuda M, Fulda S, Fusco C,**
735 **Gabryel B, Gaestel M, Gailly P, Gajewska M, Galadari S, Galili G, Galindo I, Galindo MF,**
736 **Galliciotti G, Galluzzi L, Galy V, Gammoh N, Gandy S, Ganesan AK, Ganesan S, Ganley**
737 **IG, Gannagé M, Gao FB, Gao F, Gao JX, García Nannig L, García Véscovi E, Garcia-**
738 **Macía M, Garcia-Ruiz C, Garg AD, Garg PK, Gargini R, Gassen NC, Gatica D, Gatti E,**
739 **Gavard J, Gavathiotis E, Ge L, Ge P, Ge S, Gean PW, Gelmetti V, Genazzani AA, Geng J,**
740 **Genschik P, Gerner L, Gestwicki JE, Gewirtz DA, Ghavami S, Ghigo E, Ghosh D,**
741 **Giammarioli AM, Giampieri F, Giampietri C, Giatromanolaki A, Gibbings DJ, Gibellini L,**
742 **Gibson SB, Ginet V, Giordano A, Giorgini F, Giovannetti E, Girardin SE, Gispert S,**
743 **Giuliano S, Gladson CL, Glavic A, Gleave M, Godefroy N, Gogal RM, Gokulan K,**
744 **Goldman GH, Goletti D, Goligorsky MS, Gomes AV, Gomes LC, Gomez H, Gomez-**
745 **Manzano C, Gómez-Sánchez R, Gonçalves DA, Goncu E, Gong Q, Gongora C, Gonzalez**
746 **CB, Gonzalez-Alegre P, Gonzalez-Cabo P, González-Polo RA, Goping IS, Gorbea C,**
747 **Gorbunov NV, Goring DR, Gorman AM, Gorski SM, Goruppi S, Goto-Yamada S, Gotor**
748 **C, Gottlieb RA, Gozes I, Gozuacik D, Graba Y, Graef M, Granato GE, Grant GD, Grant S,**
749 **Gravina GL, Green DR, Greenhough A, Greenwood MT, Grimaldi B, Gros F, Grose C,**
750 **Groulx JF, Gruber F, Grumati P, Grune T, Guan JL, Guan KL, Guerra B, Guillen C,**
751 **Gulshan K, Gunst J, Guo C, Guo L, Guo M, Guo W, Guo XG, Gust AA, Gustafsson Å,**

752 Gutierrez E, Gutierrez MG, Gwak HS, Haas A, Haber JE, Hadano S, Hagedorn M, Hahn
753 DR, Halayko AJ, Hamacher-Brady A, Hamada K, Hamai A, Hamann A, Hamasaki M,
754 Hamer I, Hamid Q, Hammond EM, Han F, Han W, Handa JT, Hanover JA, Hansen M,
755 Harada M, Harhaji-Trajkovic L, Harper JW, Harrath AH, Harris AL, Harris J, Hasler U,
756 Hasselblatt P, Hasui K, Hawley RG, Hawley TS, He C, He CY, He F, He G, He RR, He XH,
757 He YW, He YY, Heath JK, Hébert MJ, Heinzen RA, Helgason GV, Hensel M, Henske EP,
758 Her C, Herman PK, Hernández A, Hernandez C, Hernández-Tiedra S, Hetz C, Hiesinger
759 PR, Higaki K, Hilfiker S, Hill BG, Hill JA, Hill WD, Hino K, Hofius D, Hofman P,
760 Höglinger GU, Höhfeld J, Holz MK, Hong Y, Hood DA, Hoozemans JJ, Hoppe T, Hsu C,
761 Hsu CY, Hsu LC, Hu D, Hu G, Hu HM, Hu H, Hu MC, Hu YC, Hu ZW, Hua F, Hua Y,
762 Huang C, Huang HL, Huang KH, Huang KY, Huang S, Huang WP, Huang YR, Huang Y,
763 Huber TB, Huebbe P, Huh WK, Hulmi JJ, Hur GM, Hurley JH, Husak Z, Hussain SN,
764 Hussain S, Hwang JJ, Hwang S, Hwang TI, Ichihara A, Imai Y, Imbriano C, Inomata M,
765 Into T, Iovane V, Iovanna JL, Iozzo RV, Ip NY, Irazoqui JE, Iribarren P, Isaka Y, Isakovic
766 AJ, Ischiropoulos H, Isenberg JS, Ishaq M, Ishida H, Ishii I, Ishmael JE, Isidoro C, Isobe
767 K, Isono E, Issazadeh-Navikas S, Itahana K, Itakura E, Ivanov AI, Iyer AK, Izquierdo JM,
768 Izumi Y, Izzo V, Jäättelä M, Jaber N, Jackson DJ, Jackson WT, Jacob TG, Jacques TS,
769 Jagannath C, Jain A, Jana NR, Jang BK, Jani A, Janji B, Jannig PR, Jansson PJ, Jean S,
770 Jendrach M, Jeon JH, Jessen N, Jeung EB, Jia K, Jia L, Jiang H, Jiang L, Jiang T, Jiang X,
771 Jiang Y, Jiménez A, Jin C, Jin H, Jin L, Jin M, Jin S, Jinwal UK, Jo EK, Johansen T,
772 Johnson DE, Johnson GV, Johnson JD, Jonasch E, Jones C, Joosten LA, Jordan J, Joseph
773 AM, Joseph B, Joubert AM, Ju D, Ju J, Juan HF, Juenemann K, Juhász G, Jung HS, Jung
774 JU, Jung YK, Jungbluth H, Justice MJ, Jutten B, Kaakoush NO, Kaarniranta K, Kaasik

775 A, Kabuta T, Kaeffer B, Kågedal K, Kahana A, Kajimura S, Kakhlon O, Kalia M,
776 Kalvakolanu DV, Kamada Y, Kambas K, Kaminsky VO, Kampinga HH, Kandouz M,
777 Kang C, Kang R, Kang TC, Kanki T, Kanneganti TD, Kanno H, Kanthasamy AG,
778 Kantorow M, Kaparakis-Liaskos M, Kapuy O, Karantza V, Karim MR, Karmakar P,
779 Kaser A, Kaushik S, Kawula T, Kaynar AM, Ke PY, Ke ZJ, Kehrl JH, Keller KE, Kemper
780 JK, Kenworthy AK, Kepp O, Kern A, Kesari S, Kessel D, Ketteler R, Kettelhut IoC,
781 Khambu B, Khan MM, Khandelwal VK, Khare S, Kiang JG, Kiger AA, Kihara A, Kim
782 AL, Kim CH, Kim DR, Kim DH, Kim EK, Kim HY, Kim HR, Kim JS, Kim JH, Kim JC,
783 Kim KW, Kim MD, Kim MM, Kim PK, Kim SW, Kim SY, Kim YS, Kim Y, Kimchi A,
784 Kimmelman AC, Kimura T, King JS, Kirkegaard K, Kirkin V, Kirshenbaum LA, Kishi S,
785 Kitajima Y, Kitamoto K, Kitaoka Y, Kitazato K, Kley RA, Klimecki WT, Klinkenberg M,
786 Klucken J, Knævelsrud H, Knecht E, Knuppertz L, Ko JL, Kobayashi S, Koch JC,
787 Koechlin-Ramonatxo C, Koenig U, Koh YH, Köhler K, Kohlwein SD, Koike M, Komatsu
788 M, Kominami E, Kong D, Kong HJ, Konstantakou EG, Kopp BT, Korcsmaros T,
789 Korhonen L, Korolchuk VI, Koshkina NV, Kou Y, Koukourakis MI, Koumenis C, Kovács
790 AL, Kovács T, Kovacs WJ, Koya D, Kraft C, Krainc D, Kramer H, Kravic-Stevovic T,
791 Krek W, Kretz-Remy C, Krick R, Krishnamurthy M, Kriston-Vizi J, Kroemer G, Kruer
792 MC, Kruger R, Ktistakis NT, Kuchitsu K, Kuhn C, Kumar AP, Kumar A, Kumar D,
793 Kumar R, Kumar S, Kundu M, Kung HJ, Kuno A, Kuo SH, Kuret J, Kurz T, Kwok T,
794 Kwon TK, Kwon YT, Kyrmizi I, La Spada AR, Lafont F, Lahm T, Lakkaraju A, Lam T,
795 Lamark T, Lancel S, Landowski TH, Lane DJ, Lane JD, Lanzi C, Lapaquette P, Lapierre
796 LR, Laporte J, Laukkarinen J, Laurie GW, Lavandero S, Lavie L, LaVoie MJ, Law BY,
797 Law HK, Law KB, Layfield R, Lazo PA, Le Cam L, Le Roch KG, Le Stunff H,

798 Leardkamolkarn V, Lecuit M, Lee BH, Lee CH, Lee EF, Lee GM, Lee HJ, Lee H, Lee JK,
799 Lee J, Lee JH, Lee M, Lee MS, Lee PJ, Lee SW, Lee SJ, Lee SY, Lee SH, Lee SS, Lee S,
800 Lee YR, Lee YJ, Lee YH, Leeuwenburgh C, Lefort S, Legouis R, Lei J, Lei QY, Leib DA,
801 Leibowitz G, Lekli I, Lemaire SD, Lemasters JJ, Lemberg MK, Lemoine A, Leng S, Lenz
802 G, Lenzi P, Lerman LO, Lettieri Barbato D, Leu JI, Leung HY, Levine B, Lewis PA,
803 Lezoualc'h F, Li C, Li F, Li FJ, Li J, Li K, Li L, Li M, Li Q, Li R, Li S, Li W, Li X, Li Y,
804 Lian J, Liang C, Liang Q, Liao Y, Liberal J, Liberski PP, Lie P, Lieberman AP, Lim HJ,
805 Lim KL, Lim K, Lima RT, Lin CS, Lin CF, Lin F, Lin FC, Lin K, Lin KH, Lin PH, Lin T,
806 Lin WW, Lin YS, Lin Y, Linden R, Lindholm D, Lindqvist LM, Lingor P, Linkermann A,
807 Liotta LA, Lipinski MM, Lira VA, Lisanti MP, Liton PB, Liu B, Liu C, Liu CF, Liu F, Liu
808 HJ, Liu J, Liu JJ, Liu JL, Liu K, Liu L, Liu Q, Liu RY, Liu S, Liu W, Liu XD, Liu X, Liu
809 XH, Liu Y, Liu Z, Liuzzi JP, Lizard G, Ljubic M, Lodhi IJ, Logue SE, Lokeshwar BL,
810 Long YC, Lonial S, Loos B, López-Otín C, López-Vicario C, Lorente M, Lorenzi PL,
811 Lőrincz P, Los M, Lotze MT, Lovat PE, Lu B, Lu J, Lu Q, Lu SM, Lu S, Lu Y, Luciano F,
812 Luckhart S, Lucocq JM, Ludovico P, Lugea A, Lukacs NW, Lum JJ, Lund AH, Luo H,
813 Luo J, Luo S, Luparello C, Lyons T, Ma J, Ma Y, Ma Z, Machado J, Machado-Santelli
814 GM, Macian F, MacIntosh GC, MacKeigan JP, Macleod KF, MacMicking JD, MacMillan-
815 Crow LA, Madeo F, Madesh M, Madrigal-Matute J, Maeda A, Maeda T, Maegawa G,
816 Maellaro E, Maes H, Magariños M, Maiese K, Maiti TK, Maiuri L, Maiuri MC, Maki CG,
817 Malli R, Malorni W, Maloyan A, Mami-Chouaib F, Man N, Mancias JD, Mandelkow EM,
818 Mandell MA, Manfredi AA, Manié SN, Manzoni C, Mao K, Mao Z, Mao ZW, Marambaud
819 P, Marconi AM, Marelja Z, Marfe G, Margeta M, Margittai E, Mari M, Mariani FV,
820 Marin C, Marinelli S, Mariño G, Markovic I, Marquez R, Martelli AM, Martens S, Martin

821 KR, Martin SJ, Martin S, Martin-Acebes MA, Martín-Sanz P, Martinand-Mari C,
822 Martinet W, Martinez J, Martinez-Lopez N, Martinez-Outschoorn U, Martínez-Velázquez
823 M, Martinez-Vicente M, Martins WK, Mashima H, Mastrianni JA, Matarese G, Matarrese
824 P, Mateo R, Matoba S, Matsumoto N, Matsushita T, Matsuura A, Matsuzawa T, Mattson
825 MP, Matus S, Maugeri N, Mauvezin C, Mayer A, Maysinger D, Mazzolini GD, McBrayer
826 MK, McCall K, McCormick C, McInerney GM, McIver SC, McKenna S, McMahan JJ,
827 McNeish IA, Mechta-Grigoriou F, Medema JP, Medina DL, Megyeri K, Mehrpour M,
828 Mehta JL, Mei Y, Meier UC, Meijer AJ, Meléndez A, Melino G, Melino S, de Melo EJ,
829 Mena MA, Meneghini MD, Menendez JA, Menezes R, Meng L, Meng LH, Meng S,
830 Menghini R, Menko AS, Menna-Barreto RF, Menon MB, Meraz-Ríos MA, Merla G,
831 Merlini L, Merlot AM, Meryk A, Meschini S, Meyer JN, Mi MT, Miao CY, Micale L,
832 Michaeli S, Michiels C, Migliaccio AR, Mihailidou AS, Mijaljica D, Mikoshiba K, Milan E,
833 Miller-Fleming L, Mills GB, Mills IG, Minakaki G, Minassian BA, Ming XF, Minibayeva
834 F, Minina EA, Mintern JD, Minucci S, Miranda-Vizuete A, Mitchell CH, Miyamoto S,
835 Miyazawa K, Mizushima N, Mnich K, Mograbi B, Mohseni S, Moita LF, Molinari M,
836 Møller AB, Mollereau B, Mollinedo F, Mongillo M, Monick MM, Montagnaro S, Montell
837 C, Moore DJ, Moore MN, Mora-Rodriguez R, Moreira PI, Morel E, Morelli MB, Moreno
838 S, Morgan MJ, Moris A, Moriyasu Y, Morrison JL, Morrison LA, Morselli E, Moscat J,
839 Moseley PL, Mostowy S, Motori E, Mottet D, Mottram JC, Moussa CE, Mpakou VE,
840 Mukhtar H, Mulcahy Levy JM, Muller S, Muñoz-Moreno R, Muñoz-Pinedo C, Münz C,
841 Murphy ME, Murray JT, Murthy A, Mysorekar IU, Nabi IR, Nabissi M, Nader GA,
842 Nagahara Y, Nagai Y, Nagata K, Nagelkerke A, Nagy P, Naidu SR, Nair S, Nakano H,
843 Nakatogawa H, Nanjundan M, Napolitano G, Naqvi NI, Nardacci R, Narendra DP, Narita

844 M, Nascimbeni AC, Natarajan R, Navegantes LC, Nawrocki ST, Nazarko TY, Nazarko
845 VY, Neill T, Neri LM, Netea MG, Netea-Maier RT, Neves BM, Ney PA, Nezis IP, Nguyen
846 HT, Nguyen HP, Nicot AS, Nilsen H, Nilsson P, Nishimura M, Nishino I, Niso-Santano M,
847 Niu H, Nixon RA, Njar VC, Noda T, Noegel AA, Nolte EM, Norberg E, Norga KK,
848 Noureini SK, Notomi S, Notterpek L, Nowikovsky K, Nukina N, Nürnberger T, O'Donnell
849 VB, O'Donovan T, O'Dwyer PJ, Oehme I, Oeste CL, Ogawa M, Ogretmen B, Ogura Y, Oh
850 YJ, Ohmuraya M, Ohshima T, Ojha R, Okamoto K, Okazaki T, Oliver FJ, Ollinger K,
851 Olsson S, Orban DP, Ordonez P, Orhon I, Orosz L, O'Rourke EJ, Orozco H, Ortega AL,
852 Ortona E, Osellame LD, Oshima J, Oshima S, Osiewacz HD, Otomo T, Otsu K, Ou JH,
853 Outeiro TF, Ouyang DY, Ouyang H, Overholtzer M, Ozbun MA, Ozdinler PH, Ozpolat B,
854 Pacelli C, Paganetti P, Page G, Pages G, Pagnini U, Pajak B, Pak SC, Pakos-Zebrucka K,
855 Pakpour N, Palková Z, Palladino F, Pallauf K, Pallet N, Palmieri M, Paludan SR, Palumbo
856 C, Palumbo S, Pampliega O, Pan H, Pan W, Panaretakis T, Pandey A, Pantazopoulou A,
857 Papackova Z, Papademetrio DL, Papassideri I, Papini A, Parajuli N, Pardo J, Parekh VV,
858 Parenti G, Park JI, Park J, Park OK, Parker R, Parlato R, Parys JB, Parzych KR, Pasquet
859 JM, Pasquier B, Pasumarthi KB, Patschan D, Patterson C, Patingre S, Pattison S, Pause
860 A, Pavenstädt H, Pavone F, Pedrozo Z, Peña FJ, Peñalva MA, Pende M, Peng J, Penna F,
861 Penninger JM, Pensalfini A, Pepe S, Pereira GJ, Pereira PC, Pérez-de la Cruz V, Pérez-
862 Pérez ME, Pérez-Rodríguez D, Pérez-Sala D, Perier C, Perl A, Perlmutter DH, Perrotta I,
863 Pervaiz S, Pesonen M, Pessin JE, Peters GJ, Petersen M, Petrache I, Petrof BJ, Petrovski
864 G, Phang JM, Piacentini M, Pierdominici M, Pierre P, Pierrefite-Carle V, Pietrocola F,
865 Pimentel-Muiños FX, Pinar M, Pineda B, Pinkas-Kramarski R, Pinti M, Pinton P, Piperdi
866 B, Piret JM, Plataniias LC, Platta HW, Plowey ED, Pöggeler S, Poirot M, Polčic P, Poletti

867 A, Poon AH, Popelka H, Popova B, Poprawa I, Poulouse SM, Poulton J, Powers SK, Powers
868 T, Pozuelo-Rubio M, Prak K, Prange R, Prescott M, Priault M, Prince S, Proia RL,
869 Proikas-Cezanne T, Prokisch H, Promponas VJ, Przyklenk K, Puertollano R, Pugazhenth
870 S, Puglielli L, Pujol A, Puyal J, Pyeon D, Qi X, Qian WB, Qin ZH, Qiu Y, Qu Z,
871 Quadrilatero J, Quinn F, Raben N, Rabinowich H, Radogna F, Ragusa MJ, Rahmani M,
872 Raina K, Ramanadham S, Ramesh R, Rami A, Randall-Demllo S, Randow F, Rao H, Rao
873 VA, Rasmussen BB, Rasse TM, Ratovitski EA, Rautou PE, Ray SK, Razani B, Reed BH,
874 Reggiori F, Rehm M, Reichert AS, Rein T, Reiner DJ, Reits E, Ren J, Ren X, Renna M,
875 Reusch JE, Revuelta JL, Reyes L, Rezaie AR, Richards RI, Richardson DR, Richetta C,
876 Riehle MA, Rihn BH, Rikihisa Y, Riley BE, Rimbach G, Rippo MR, Ritis K, Rizzi F, Rizzo
877 E, Roach PJ, Robbins J, Roberge M, Roca G, Roccheri MC, Rocha S, Rodrigues CM,
878 Rodríguez CI, de Cordoba SR, Rodriguez-Muela N, Roelofs J, Rogov VV, Rohn TT,
879 Rohrer B, Romanelli D, Romani L, Romano PS, Roncero MI, Rosa JL, Rosello A, Rosen
880 KV, Rosenstiel P, Rost-Roszkowska M, Roth KA, Roué G, Rouis M, Rouschop KM, Ruan
881 DT, Ruano D, Rubinsztein DC, Rucker EB, Rudich A, Rudolf E, Rudolf R, Ruegg MA,
882 Ruiz-Roldan C, Ruparelia AA, Rusmini P, Russ DW, Russo GL, Russo G, Russo R, Rusten
883 TE, Ryabovol V, Ryan KM, Ryter SW, Sabatini DM, Sacher M, Sachse C, Sack MN,
884 Sadoshima J, Saftig P, Sagi-Eisenberg R, Sahni S, Saikumar P, Saito T, Saitoh T, Sakakura
885 K, Sakoh-Nakatogawa M, Sakuraba Y, Salazar-Roa M, Salomoni P, Saluja AK, Salvaterra
886 PM, Salvioli R, Samali A, Sanchez AM, Sánchez-Alcázar JA, Sanchez-Prieto R, Sandri M,
887 Sanjuan MA, Santaguida S, Santambrogio L, Santoni G, Dos Santos CN, Saran S, Sardiello
888 M, Sargent G, Sarkar P, Sarkar S, Sarrias MR, Sarwal MM, Sasakawa C, Sasaki M, Sass
889 M, Sato K, Sato M, Satriano J, Savaraj N, Saveljeva S, Schaefer L, Schaible UE, Scharl M,

890 Schatzl HM, Schekman R, Scheper W, Schiavi A, Schipper HM, Schmeisser H, Schmidt J,
891 Schmitz I, Schneider BE, Schneider EM, Schneider JL, Schon EA, Schönenberger MJ,
892 Schönthal AH, Schorderet DF, Schröder B, Schuck S, Schulze RJ, Schwarten M, Schwarz
893 TL, Sciarretta S, Scotto K, Scovassi AI, Screatton RA, Screen M, Seca H, Sedej S, Segatori
894 L, Segev N, Seglen PO, Seguí-Simarro JM, Segura-Aguilar J, Seki E, Sell C, Seiliez I,
895 Semenkovich CF, Semenza GL, Sen U, Serra AL, Serrano-Puebla A, Sesaki H, Setoguchi
896 T, Settembre C, Shacka JJ, Shajahan-Haq AN, Shapiro IM, Sharma S, She H, Shen CK,
897 Shen CC, Shen HM, Shen S, Shen W, Sheng R, Sheng X, Sheng ZH, Shepherd TG, Shi J,
898 Shi Q, Shi Y, Shibutani S, Shibuya K, Shidoji Y, Shieh JJ, Shih CM, Shimada Y, Shimizu
899 S, Shin DW, Shinohara ML, Shintani M, Shintani T, Shioi T, Shirabe K, Shiri-Sverdlov R,
900 Shirihai O, Shore GC, Shu CW, Shukla D, Sibirny AA, Sica V, Sigurdson CJ, Sigurdsson
901 EM, Sijwali PS, Sikorska B, Silveira WA, Silvente-Poirot S, Silverman GA, Simak J,
902 Simmet T, Simon AK, Simon HU, Simone C, Simons M, Simonsen A, Singh R, Singh SV,
903 Singh SK, Sinha D, Sinha S, Sinicrope FA, Sirko A, Sirohi K, Sishi BJ, Sittler A, Siu PM,
904 Sivridis E, Skwarska A, Slack R, Slaninová I, Slavov N, Smaili SS, Smalley KS, Smith DR,
905 Soenen SJ, Soleimanpour SA, Solhaug A, Somasundaram K, Son JH, Sonawane A, Song C,
906 Song F, Song HK, Song JX, Song W, Soo KY, Sood AK, Soong TW, Soontornniyomkij V,
907 Sorice M, Sotgia F, Soto-Pantoja DR, Sotthibundhu A, Sousa MJ, Spaink HP, Span PN,
908 Spang A, Sparks JD, Speck PG, Spector SA, Spies CD, Springer W, Clair DS, Stacchiotti
909 A, Staels B, Stang MT, Starczynowski DT, Starokadomskyy P, Steegborn C, Steele JW,
910 Stefanis L, Steffan J, Stellrecht CM, Stenmark H, Stepkowski TM, Stern ST, Stevens C,
911 Stockwell BR, Stoka V, Storchova Z, Stork B, Stratoulas V, Stravopodis DJ, Strnad P,
912 Strohecker AM, Ström AL, Stromhaug P, Stulik J, Su YX, Su Z, Subauste CS,

913 Subramaniam S, Sue CM, Suh SW, Sui X, Sukserree S, Sulzer D, Sun FL, Sun J, Sun SY,
914 Sun Y, Sundaramoorthy V, Sung J, Suzuki H, Suzuki K, Suzuki N, Suzuki T, Suzuki YJ,
915 Swanson MS, Swanton C, Swärd K, Swarup G, Sweeney ST, Sylvester PW, Szatmari Z,
916 Szegezdi E, Szlosarek PW, Taegtmeier H, Tafani M, Taillebourg E, Tait SW, Takacs-
917 Vellai K, Takahashi Y, Takáts S, Takemura G, Takigawa N, Talbot NJ, Tamagno E,
918 Tamburini J, Tan CP, Tan L, Tan ML, Tan M, Tan YJ, Tanaka K, Tanaka M, Tang D,
919 Tang G, Tanida I, Tanji K, Tannous BA, Tapia JA, Tasset-Cuevas I, Tatar M, Tavassoly I,
920 Tavernarakis N, Taylor A, Taylor GS, Taylor GA, Taylor JP, Taylor MJ, Tchetina EV,
921 Tee AR, Teixeira-Clerc F, Telang S, Tencomnao T, Teng BB, Teng RJ, Terro F,
922 Tettamanti G, Theiss AL, Theron AE, Thomas KJ, Thomé MP, Thomes PG, Thorburn A,
923 Thorner J, Thum T, Thumm M, Thurston TL, Tian L, Till A, Ting JP, Titorenko VI,
924 Toker L, Toldo S, Tooze SA, Topisirovic I, Torgersen ML, Torosantucci L, Torriglia A,
925 Torrisi MR, Tournier C, Towns R, Trajkovic V, Travassos LH, Triola G, Tripathi DN,
926 Trisciuglio D, Troncoso R, Trougakos IP, Truttmann AC, Tsai KJ, Tschan MP, Tseng
927 YH, Tsukuba T, Tsung A, Tsvetkov AS, Tu S, Tuan HY, Tucci M, Tumbarello DA, Turk
928 B, Turk V, Turner RF, Tveita AA, Tyagi SC, Ubukata M, Uchiyama Y, Udelnow A, Ueno
929 T, Umekawa M, Umemiya-Shirafuji R, Underwood BR, Ungermann C, Ureshino RP,
930 Ushioda R, Uversky VN, Uzcátegui NL, Vaccari T, Vaccaro MI, Váchová L,
931 Vakifahmetoglu-Norberg H, Valdor R, Valente EM, Vallette F, Valverde AM, Van den
932 Berghe G, Van Den Bosch L, van den Brink GR, van der Goot FG, van der Klei IJ, van der
933 Laan LJ, van Doorn WG, van Egmond M, van Golen KL, Van Kaer L, van Lookeren
934 Campagne M, Vandenabeele P, Vandenberghe W, Vanhorebeek I, Varela-Nieto I,
935 Vasconcelos MH, Vasko R, Vavvas DG, Vega-Naredo I, Velasco G, Velentzas AD,

936 Velentzas PD, Vellai T, Vellenga E, Vendelbo MH, Venkatachalam K, Ventura N, Ventura
937 S, Veras PS, Verdier M, Vertessy BG, Viale A, Vidal M, Vieira HL, Vierstra RD,
938 Vigneswaran N, Vij N, Vila M, Villar M, Villar VH, Villarroya J, Vindis C, Viola G,
939 Viscomi MT, Vitale G, Vogl DT, Voitsekhovskaja OV, von Haefen C, von Schwarzenberg
940 K, Voth DE, Vouret-Craviari V, Vuori K, Vyas JM, Waeber C, Walker CL, Walker MJ,
941 Walter J, Wan L, Wan X, Wang B, Wang C, Wang CY, Wang D, Wang F, Wang G, Wang
942 HJ, Wang H, Wang HG, Wang HD, Wang J, Wang M, Wang MQ, Wang PY, Wang P,
943 Wang RC, Wang S, Wang TF, Wang X, Wang XJ, Wang XW, Wang Y, Wang YJ, Wang
944 YT, Wang ZN, Wappner P, Ward C, Ward DM, Warnes G, Watada H, Watanabe Y,
945 Watase K, Weaver TE, Weekes CD, Wei J, Weide T, Weihl CC, Weindl G, Weis SN, Wen
946 L, Wen X, Wen Y, Westermann B, Weyand CM, White AR, White E, Whitton JL,
947 Whitworth AJ, Wiels J, Wild F, Wildenberg ME, Wileman T, Wilkinson DS, Wilkinson S,
948 Willbold D, Williams C, Williams K, Williamson PR, Winklhofer KF, Witkin SS,
949 Wohlgemuth SE, Wollert T, Wolvetang EJ, Wong E, Wong GW, Wong RW, Wong VK,
950 Woodcock EA, Wright KL, Wu C, Wu D, Wu GS, Wu J, Wu M, Wu S, Wu WK, Wu Y,
951 Wu Z, Xavier CP, Xavier RJ, Xia GX, Xia T, Xia W, Xia Y, Xiao H, Xiao J, Xiao S, Xiao
952 W, Xie CM, Xie Z, Xilouri M, Xiong Y, Xu C, Xu F, Xu H, Xu J, Xu L, Xu X, Xu Y, Xu
953 ZX, Xu Z, Xue Y, Yamada T, Yamamoto A, Yamanaka K, Yamashina S, Yamashiro S,
954 Yan B, Yan X, Yan Z, Yanagi Y, Yang DS, Yang JM, Yang L, Yang M, Yang PM, Yang P,
955 Yang Q, Yang W, Yang WY, Yang X, Yang Y, Yang Z, Yao MC, Yao PJ, Yao X, Yao Z,
956 Yasui LS, Ye M, Yedvobnick B, Yeganeh B, Yeh ES, Yeyati PL, Yi F, Yi L, Yin XM, Yip
957 CK, Yoo YM, Yoo YH, Yoon SY, Yoshida K, Yoshimori T, Young KH, Yu H, Yu JJ, Yu
958 JT, Yu J, Yu L, Yu WH, Yu XF, Yu Z, Yuan J, Yuan ZM, Yue BY, Yue J, Yue Z, Zacks

959 **DN, Zacksenhaus E, Zaffaroni N, Zaglia T, Zakeri Z, Zecchini V, Zeng J, Zeng M, Zeng Q,**
960 **Zervos AS, Zhang DD, Zhang F, Zhang G, Zhang GC, Zhang H, Zhang J, Zhang JP,**
961 **Zhang L, Zhang MY, Zhang X, Zhang XD, Zhang Y, Zhao M, Zhao WL, Zhao X, Zhao**
962 **YG, Zhao Y, Zhao YX, Zhao Z, Zhao ZJ, Zheng D, Zheng XL, Zheng X, Zhivotovsky B,**
963 **Zhong Q, Zhou GZ, Zhou G, Zhou H, Zhou SF, Zhou XJ, Zhu H, Zhu WG, Zhu W, Zhu**
964 **XF, Zhu Y, Zhuang SM, Zhuang X, Ziparo E, Zois CE, Zoladek T, Zong WX, Zorzano A,**
965 **and Zughaier SM.** Guidelines for the use and interpretation of assays for monitoring autophagy
966 (3rd edition). *Autophagy* 12: 1-222, 2016.

967 39. **Knarr M, Nagaraj AB, Kwiatkowski LJ, and DiFeo A.** miR-181a modulates circadian
968 rhythm in immortalized bone marrow and adipose derived stromal cells and promotes
969 differentiation through the regulation of PER3. *Sci Rep* 9: 307, 2019.

970 40. **Kubli DA, and Gustafsson Å.** Mitochondria and mitophagy: the yin and yang of cell
971 death control. *Circ Res* 111: 1208-1221, 2012.

972 41. **Lee C, Etchegaray JP, Cagampang FR, Loudon AS, and Reppert SM.**
973 Posttranslational mechanisms regulate the mammalian circadian clock. *Cell* 107: 855-867, 2001.

974 42. **Lee D, and Goldberg AL.** SIRT1 protein, by blocking the activities of transcription
975 factors FoxO1 and FoxO3, inhibits muscle atrophy and promotes muscle growth. *J Biol Chem*
976 288: 30515-30526, 2013.

977 43. **Lee DE, Brown JL, Rosa ME, Brown LA, Perry RA, Wiggs MP, Nilsson MI, Crouse**
978 **SF, Fluckey JD, Washington TA, and Greene NP.** microRNA-16 Is Downregulated During
979 Insulin Resistance and Controls Skeletal Muscle Protein Accretion. *J Cell Biochem* 117: 1775-
980 1787, 2016.

- 981 44. **Lin J, Wu H, Tarr PT, Zhang CY, Wu Z, Boss O, Michael LF, Puigserver P, Isotani**
982 **E, Olson EN, Lowell BB, Bassel-Duby R, and Spiegelman BM.** Transcriptional co-activator
983 PGC-1 alpha drives the formation of slow-twitch muscle fibres. *Nature* 418: 797-801, 2002.
- 984 45. **McCarthy JJ, Andrews JL, McDearmon EL, Campbell KS, Barber BK, Miller BH,**
985 **Walker JR, Hogenesch JB, Takahashi JS, and Esser KA.** Identification of the circadian
986 transcriptome in adult mouse skeletal muscle. *Physiol Genomics* 31: 86-95, 2007.
- 987 46. **Mobley CB, Mumford PW, Kephart WC, Conover CF, Beggs LA, Balazs A, Yarrow**
988 **JF, Borst SE, Beck DT, and Roberts MD.** Effects of testosterone treatment on markers of
989 skeletal muscle ribosome biogenesis. *Andrologia* 48: 967-977, 2016.
- 990 47. **Nahapetyan H, Moulis M, Grousset E, Faccini J, Graziade MH, Mucher E, Elbaz M,**
991 **Martinet W, and Vindis C.** Altered mitochondrial quality control in Atg7-deficient VSMCs
992 promotes enhanced apoptosis and is linked to unstable atherosclerotic plaque phenotype. *Cell*
993 *Death Dis* 10: 119, 2019.
- 994 48. **Neufeld-Cohen A, Robles MS, Aviram R, Manella G, Adamovich Y, Ladeux B, Nir**
995 **D, Rouso-Noori L, Kuperman Y, Golik M, Mann M, and Asher G.** Circadian control of
996 oscillations in mitochondrial rate-limiting enzymes and nutrient utilization by PERIOD proteins.
997 *Proc Natl Acad Sci U S A* 113: E1673-1682, 2016.
- 998 49. **Nguyen TN, Padman BS, and Lazarou M.** Deciphering the Molecular Signals of
999 PINK1/Parkin Mitophagy. *Trends Cell Biol* 26: 733-744, 2016.
- 1000 50. **Ni HM, Williams JA, and Ding WX.** Mitochondrial dynamics and mitochondrial
1001 quality control. *Redox Biol* 4: 6-13, 2015.
- 1002 51. **Ophoff J, Van Proeyen K, Callewaert F, De Gendt K, De Bock K, Vanden Bosch A,**
1003 **Verhoeven G, Hespel P, and Vanderschueren D.** Androgen signaling in myocytes contributes

1004 to the maintenance of muscle mass and fiber type regulation but not to muscle strength or
1005 fatigue. *Endocrinology* 150: 3558-3566, 2009.

1006 52. **Rana K, Chiu MW, Russell PK, Skinner JP, Lee NK, Fam BC, Zajac JD, and**
1007 **MacLean HE.** Muscle-specific androgen receptor deletion shows limited actions in myoblasts
1008 but not in myofibers in different muscles in vivo. *J Mol Endocrinol* 57: 125-138, 2016.

1009 53. **Romanello V, and Sandri M.** Mitochondrial Quality Control and Muscle Mass
1010 Maintenance. *Front Physiol* 6: 422, 2015.

1011 54. **Rossetti ML, Fukuda DH, and Gordon BS.** Androgens induce growth of the limb
1012 skeletal muscles in a rapamycin-insensitive manner. *Am J Physiol Regul Integr Comp Physiol*
1013 2018.

1014 55. **Rossetti ML, and Gordon BS.** The role of androgens in the regulation of muscle
1015 oxidative capacity following aerobic exercise training. *Appl Physiol Nutr Metab* 42: 1001-1007,
1016 2017.

1017 56. **Rossetti ML, Steiner JL, and Gordon BS.** Increased mitochondrial turnover in the
1018 skeletal muscle of fasted, castrated mice is related to the magnitude of autophagy activation and
1019 muscle atrophy. *Mol Cell Endocrinol* 2018.

1020 57. **Sahar S, Zocchi L, Kinoshita C, Borrelli E, and Sassone-Corsi P.** Regulation of
1021 BMAL1 protein stability and circadian function by GSK3beta-mediated phosphorylation. *PLoS*
1022 *One* 5: e8561, 2010.

1023 58. **Schroder EA, Harfmann BD, Zhang X, Srikuea R, England JH, Hodge BA, Wen Y,**
1024 **Riley LA, Yu Q, Christie A, Smith JD, Seward T, Wolf Horrell EM, Mula J, Peterson CA,**
1025 **Butterfield TA, and Esser KA.** Intrinsic muscle clock is necessary for musculoskeletal health. *J*
1026 *Physiol* 593: 5387-5404, 2015.

- 1027 59. **Serra C, Sandor NL, Jang H, Lee D, Toraldo G, Guarneri T, Wong S, Zhang A,**
1028 **Guo W, Jasuja R, and Bhasin S.** The effects of testosterone deprivation and supplementation
1029 on proteasomal and autophagy activity in the skeletal muscle of the male mouse: differential
1030 effects on high-androgen responder and low-androgen responder muscle groups. *Endocrinology*
1031 154: 4594-4606, 2013.
- 1032 60. **Shen Q, Li J, Mai J, Zhang Z, Fisher A, Wu X, Li Z, Ramirez MR, Chen S, and**
1033 **Shen H.** Sensitizing non-small cell lung cancer to BCL-xL-targeted apoptosis. *Cell Death Dis* 9:
1034 986, 2018.
- 1035 61. **Smuder AJ, Sollanek KJ, Nelson WB, Min K, Talbert EE, Kavazis AN, Hudson**
1036 **MB, Sandri M, Szeto HH, and Powers SK.** Crosstalk between autophagy and oxidative stress
1037 regulates proteolysis in the diaphragm during mechanical ventilation. *Free Radic Biol Med* 115:
1038 179-190, 2018.
- 1039 62. **Srikanthan P, Horwich TB, and Tseng CH.** Relation of Muscle Mass and Fat Mass to
1040 Cardiovascular Disease Mortality. *Am J Cardiol* 117: 1355-1360, 2016.
- 1041 63. **Srikanthan P, and Karlamangla AS.** Muscle mass index as a predictor of longevity in
1042 older adults. *Am J Med* 127: 547-553, 2014.
- 1043 64. **Steiner JL, Fukuda DH, Rossetti ML, Hoffman JR, and Gordon BS.** Castration alters
1044 protein balance after high-frequency muscle contraction. *J Appl Physiol (1985)* 122: 264-272,
1045 2017.
- 1046 65. **Suliman HB, and Piantadosi CA.** Mitochondrial Quality Control as a Therapeutic
1047 Target. *Pharmacol Rev* 68: 20-48, 2016.
- 1048 66. **Szeszycki EE.** Testosterone replacement increases fat-free mass and muscle size in
1049 hypogonadal men. *JPEN J Parenter Enteral Nutr* 21: 241-242, 1997.

- 1050 67. **Ueberschlag-Pitiot V, Stantzou A, Messéant J, Lemaitre M, Owens DJ, Noirez P,**
1051 **Roy P, Agbulut O, Metzger D, and Ferry A.** Gonad-related factors promote muscle
1052 performance gain during postnatal development in male and female mice. *Am J Physiol*
1053 *Endocrinol Metab* 313: E12-E25, 2017.
- 1054 68. **Urban RJ, Bodenbun YH, Gilkison C, Foxworth J, Coggan AR, Wolfe RR, and**
1055 **Ferrando A.** Testosterone administration to elderly men increases skeletal muscle strength and
1056 protein synthesis. *Am J Physiol* 269: E820-826, 1995.
- 1057 69. **Vanselow K, Vanselow JT, Westermark PO, Reischl S, Maier B, Korte T,**
1058 **Herrmann A, Herzel H, Schlosser A, and Kramer A.** Differential effects of PER2
1059 phosphorylation: molecular basis for the human familial advanced sleep phase syndrome
1060 (FASPS). *Genes Dev* 20: 2660-2672, 2006.
- 1061 70. **Wang Z, Li L, and Wang Y.** Effects of Per2 overexpression on growth inhibition and
1062 metastasis, and on MTA1, nm23-H1 and the autophagy-associated PI3K/PKB signaling pathway
1063 in nude mice xenograft models of ovarian cancer. *Mol Med Rep* 13: 4561-4568, 2016.
- 1064 71. **White JP, Gao S, Puppa MJ, Sato S, Welle SL, and Carson JA.** Testosterone
1065 regulation of Akt/mTORC1/FoxO3a signaling in skeletal muscle. *Mol Cell Endocrinol* 365: 174-
1066 186, 2013.
- 1067 72. **White JP, Puppa MJ, Narsale A, and Carson JA.** Characterization of the male
1068 *ApcMin*⁺ mouse as a hypogonadism model related to cancer cachexia. *Biol Open* 2: 1346-1353,
1069 2013.
- 1070 73. **Youle RJ, and van der Blik AM.** Mitochondrial fission, fusion, and stress. *Science*
1071 337: 1062-1065, 2012.

- 1072 74. **Zhang S, Eitan E, and Mattson MP.** Early involvement of lysosome dysfunction in the
1073 degeneration of cerebral cortical neurons caused by the lipid peroxidation product 4-
1074 hydroxynonenal. *J Neurochem* 140: 941-954, 2017.
- 1075 75. **Zhang T, Xue L, Li L, Tang C, Wan Z, Wang R, Tan J, Tan Y, Han H, Tian R,**
1076 **Billiar TR, Tao WA, and Zhang Z.** BNIP3 Protein Suppresses PINK1 Kinase Proteolytic
1077 Cleavage to Promote Mitophagy. *J Biol Chem* 291: 21616-21629, 2016.
- 1078 76. **Zhou B, Li C, Qi W, Zhang Y, Zhang F, Wu JX, Hu YN, Wu DM, Liu Y, Yan TT,**
1079 **Jing Q, Liu MF, and Zhai QW.** Downregulation of miR-181a upregulates sirtuin-1 (SIRT1)
1080 and improves hepatic insulin sensitivity. *Diabetologia* 55: 2032-2043, 2012.
- 1081 77. **Zou T, Chen D, Yang Q, Wang B, Zhu MJ, Nathanielsz PW, and Du M.** Resveratrol
1082 supplementation of high-fat diet-fed pregnant mice promotes brown and beige adipocyte
1083 development and prevents obesity in male offspring. *J Physiol* 595: 1547-1562, 2017.

1084

1085 **FIGURE LEGENDS**

1086

1087 Figure 1: Characterization of changes to the core clock gene expression in the limb skeletal
1088 muscle following androgen depletion. (A-D) Microarray analysis was confirmed by measuring
1089 the relative mRNA content of *Bmall*, and *Per1-3* in the TA of sham and castrated mice by RT-
1090 PCR (N = 7/8 per group for microarray validation). These samples were collected between
1091 1300-1500 hr. (E-J) The circadian expression patterns of *Bmall*, *Clock*, *Per1-3*, and *Cry1*
1092 mRNA were determined in the TA of sham and castrated mice by RT-PCR N = 3/group/time
1093 point for circadian measurements. Student's *t*-test was used to confirm microarray analysis.
1094 Two-way ANOVA was used to assess changes in circadian expression patterns. ME: Main

1095 Effect. * Significantly different than the mean value in the Sham group, or significantly different
1096 than the Sham value at the given circadian time. $P \leq 0.05$ for all other analysis.

1097

1098 Figure 2: Assessment of core clock function in the limb muscle following androgen depletion.
1099 (A-E) The circadian expression pattern of various clock-controlled genes including *ROR α* , *Rev-*
1100 *Erba*, *MyoD*, *Dbp*, and *MAFbx* were determined in the TA of sham and castrated mice by RT-
1101 PCR. N = 3/group/time point for circadian measurements. Student's *t*-test was used to confirm
1102 microarray analysis. Two-way ANOVA was used to assess changes in circadian expression
1103 patterns. ME: Main Effect. * Significantly different than the Sham value at the given circadian
1104 time. $P \leq 0.05$ for all other analysis.

1105

1106 Figure 3: Assessment of circadian expression patterns for genes involved with mitochondrial
1107 quality control in the limb skeletal muscle following androgen depletion. The circadian
1108 expression pattern of genes involved with (A-B) mitochondrial fission, (C-E) mitochondrial
1109 fusion, (F-H) mitochondrial biogenesis, and (I-K) mitophagy were determined in the TA of sham
1110 and castrated mice by RT-PCR. Two-way ANOVA was used to assess circadian expression
1111 patterns. N = 3/group/time point for circadian measurements. ME: Main Effect. * Significantly
1112 different than Sham value at the given circadian time. $P \leq 0.05$ for all other analysis.

1113

1114 Figure 4: Assessment of mitophagy and autophagy activation patterns in the limb skeletal
1115 muscle following androgen depletion. (A-C) The circadian protein expression patterns for
1116 mitophagy related proteins were determined in the TA of sham and castrated mice by Western
1117 blot analysis. (D-F) The circadian protein expression patterns of the LC3 II/I ratio, LC3 I, and

1118 LC3 II were determined in the TA of sham and castrated mice by Western blot analysis. (G) The
1119 circadian expression pattern for *LC3B* mRNA was determined in the TA of sham and castrated
1120 mice by RT-PCR. For Western blot analysis, an equal amount of protein from each sample
1121 within a group (N=3 sham or castrated) at each time point was pooled together for analysis. If a
1122 visual difference in the expression patterns across ≥ 3 consecutive time points was observed,
1123 differences in the mean pixel intensity values obtained from the ≥ 3 time points for each group
1124 (sham or castrated) were assessed statistically. (H) Western blot. Black line on blot is used to
1125 visually separate the sham and castrated groups. Two-way ANOVA was used to assess the
1126 circadian expression pattern of *LC3B* mRNA. Student's *t*-test was used to assess difference in
1127 the pixel intensity of ≥ 3 consecutive time points of protein in the TA. N = 3/group/time point
1128 for circadian measurement of *LC3B* mRNA. ME: Main Effect; CT: Circadian Time. *
1129 Significant difference from ≥ 3 consecutive time points between groups under the solid black
1130 line. $P \leq 0.05$ for analysis.

1131
1132 Figure 5: Assessment of mitochondrial protein expression patterns in the limb skeletal muscle
1133 following androgen depletion. The circadian expression patterns for (A) COX IV, (B) VDAC,
1134 (C) Bcl-xL, and (D) 4-HNE were determined in the TA of sham and castrated mice by Western
1135 blot analysis. (E) Western blot. Black line on blot is used to visually separate the sham and
1136 castrated groups. For Western blot analysis, an equal amount of protein from each sample within
1137 a group (N=3 sham or castrated) at each time point was pooled together for analysis. If a visual
1138 difference in the expression patterns across ≥ 3 consecutive time points was observed, differences
1139 in the mean pixel intensity values obtained from the ≥ 3 time points for each group (sham or
1140 castrated) were assessed statistically. Student's *t*-test was used to assess difference in the pixel

1141 intensity of ≥ 3 consecutive time points of protein in the TA. CT: Circadian Time; NS: Non-
1142 Specific. The black arrows indicate non-specific reactivity by the anti-mouse secondary
1143 antibody. For illustrative purposes only, the lanes of the 4 HNE blot were made vertical in
1144 Adobe Photoshop after quantification. * Significant difference from ≥ 3 consecutive time points
1145 between groups under the solid black line. $P \leq 0.05$ for analysis.

1146

1147 Figure 6: Assessment of Bmal1 regulation in the limb skeletal muscle following androgen
1148 depletion. The circadian protein expression pattern of (A) Bmal1 was determined in the TA of
1149 sham and castrated mice by Western blot analysis. (B) The enrichment of Bmal1 protein in the
1150 cytosolic and nuclear-enriched fractions was determined in the gastrocnemius of sham and
1151 castrated mice by Western blot analysis. The circadian patterns for the ratio of phosphorylated to
1152 total protein for (C) GSK3 β (Ser9) and (D) Akt (Ser473) were determined in the TA of sham and
1153 castrated mice by Western blot analysis. (E) Western blot. Black line on blot is used to visually
1154 separate the sham and castrated groups. For Western blot analysis, an equal amount of protein
1155 from each sample within a group (N=3 sham or castrated) at each time point was pooled together
1156 for analysis. If a visual difference in the expression patterns across ≥ 3 consecutive time points
1157 was observed, differences in the mean pixel intensity values obtained from the ≥ 3 time points for
1158 each group (sham or castrated) were assessed statistically. Student's *t*-test was used to assess
1159 difference in the pixel intensity of ≥ 3 consecutive time points of protein in the TA. CT:
1160 Circadian Time; Exp: Exposure. * Significant difference from ≥ 3 consecutive time points
1161 between groups under the solid black line. $P \leq 0.05$ for all analysis.

1162

1163 Figure 7: Assessment of Per2 regulation in the limb skeletal muscle following androgen
 1164 depletion. The circadian protein expression pattern of (A) Per2, (B) Per2 Lower Band, and (C)
 1165 Sirt1 were assessed by Western blot analysis. For Western blot analysis, an equal amount of
 1166 protein from each sample within a group (N=3 sham or castrated) at each time point was pooled
 1167 together for analysis. If a visual difference in the expression patterns across ≥ 3 consecutive time
 1168 points was observed, differences in the mean pixel intensity values obtained from the ≥ 3 time
 1169 points for each group (sham or castrated) were assessed statistically. Student's *t*-test was used to
 1170 assess difference in the pixel intensity of ≥ 3 consecutive time points of protein in the TA. The
 1171 circadian expression patterns for (D) *Sirt1* mRNA and (E) *miR-181a* were determined in the TA
 1172 of sham and castrated mice by RT-PCR analysis. N = 3/group/time point. Two-way ANOVA
 1173 was used to assess circadian expression patterns of each RNA. (F) Western blot. Black line on
 1174 blot is used to visually separate the sham and castrated groups. ME: Main Effect, CT: Circadian
 1175 Time. * Significant difference from ≥ 3 consecutive time points between groups under the solid
 1176 black line (Western blots) or significantly different than Sham values at the given circadian time
 1177 (RT-PCR). $P \leq 0.05$ for all analysis.

1178

1179 Figure 8: Theoretical model for the androgen-mediated regulation of limb muscle mass.

1180

1181

1182 Table 1: Primer sequences for RT-PCR using Sybr Green

Gene Symbol	Forward (5'-3')	Reverse (5'-3')	Amplicon Size (bp)
<i>Bmal1</i>	TGGAGGGACTCCAGACATTC	TTGCTGCCTCATCGTTA CTG	173
<i>Per1</i>	GTCCCCTGGTCCTCTACACA	GCCCGAGATTCAATGAA GAG	159

<i>Per2</i>	AGCCACCCTGAAAAGGAAG T	GGTGAGGGACACCACA CTCT	184
<i>Per3</i>	GTCGAGAGGAGGTGCTGAA G	TCTGTCTTCACAGGCGA CAC	173
<i>Rev-Erba</i>	GGCACCTGCCAACAGTCTA	GCTGAGAAAGGTCACG GAAG	197
<i>RORa</i>	GGAAGAGTTTGTGTTCTATG CACC	TTCCATCTTCTCGGTGGT TC	177
<i>Cry1</i>	TTCACTGCTACTGCCCTGTG	CACTTGGCAACCTTCTG GAT	151
<i>MyoD</i>	TACCCAAGGTGGAGATCCTG	CATCATGCCATCAGAGC AGT	200
<i>DBP</i>	TCTAGGGACACACCCAGTCC	TGGTTGAGGCTTCAGTT CCT	159
<i>RPLP0</i>	CAACCCAGCTCTGGAGAAA C	GTTCTGAGCTGGCACAG TGA	169
<i>Drp1</i>	AGGAACCAACAACAGGCAA C	TCACAATCTCGCTGTTC TCG	190
<i>Fis1</i>	AAGTATGTGCGAGGGCTGTT	ACAGCCAGTCCAATGAG TCC	167
<i>Opal</i>	GATGACACGCTCTCCAGTGA	TCGGGGCTAACAGTACA ACC	177
<i>Mfn1</i>	GCTGTCAGAGCCCATCTTTC	CAGCCACTGTTTTCCA AAT	195
<i>Mfn2</i>	AGCGCCAGTTTGTGGAATAC	CTTTCTTGTTTCATGGCA GCA	177
<i>PGC1-α</i>	AAGACGGATTGCCCTCATTT	AGTGCTAAGACCGCTGC ATT	191
<i>Sirt1</i>	AGTTCCAGCCGTCTCTGTGT	CTCCACGAACAGCTTCA CAA	198
<i>GAPDH</i>	GTTGTCTCCTGCGACTTCA	TGCTGTAGCCGTATTCA TTG	124
<i>ID1</i>	TACGACATGAACGGCTGCTA	GTGGTCCCAGCTTCAGA CTC	155

1183

1184 Table 2: Top 5 Functional Gene Categories altered by castration.

Functional Category	# of Genes	P-Value
Polyamine biosynthesis	3	0.0011
Biological Rhythms	5	0.0019

Receptor	22	0.0021
Olfaction	13	0.0030
Decarboxylase	3	0.0034

1185

1186

1187 Table 3: Top 5 KEGG Pathways altered by castration.

KEGG Pathway	# of Genes	<i>P</i> -Value
Glutathione metabolism	4	0.0037
Systemic lupus erythematosus	5	0.0095
Circadian rhythm	3	0.013
Herpes simplex infection	5	0.030
Arginine and proline metabolism	3	0.032

1188

1189

1190

1191 Table 4: RT-PCR confirmation of the molecular clock/circadian genes identified via microarray
 1192 (N =7-8 per group).

Gene Symbol	Fold Change (Castrated vs. Sham)	<i>P</i> -Value	95% Confidence Interval
<i>Bmal1</i>	-0.57351	0.0102	-0.985 to -0.1609
<i>ID1</i>	1.8576	0.0327	1.08249 to 2.633
<i>Per2</i>	3.27	<0.0001	2.598 to 3.937
<i>Per3</i>	3.062	<0.0001	2.467 to 3.658
<i>Ppargc1a</i>	1.8999	0.0269	1.1203 to 2.68

1193

Note: *Ppargc1a* gene expression from this data set has been reported previously (56).

1194

1195 Table 5: Muscle Mass and Tibia Length

	Sham (N = 18)	Castrated (N = 18)
Tibialis Anterior (mg)	50.98 ± 0.82	42.60 ± 1.18*
Gastrocnemius (mg)	140.53 ± 1.57	130.66 ± 1.60*
Plantaris (mg)	22.73 ± 0.52	20.06 ± 0.48*
Soleus (mg)	9.79 ± 0.20	8.58 ± 0.21*
Tibia Length (mm)	17.39 ± 0.10	17.17 ± 0.09

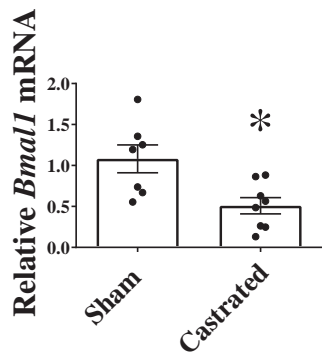
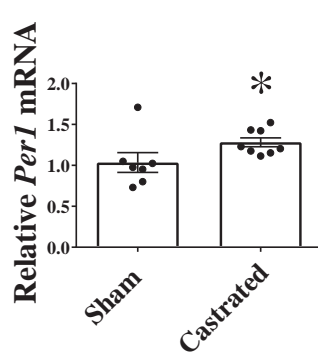
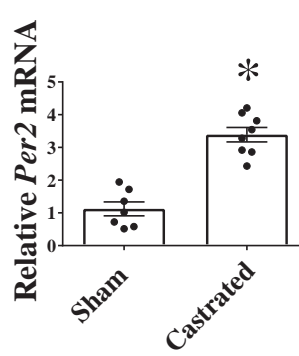
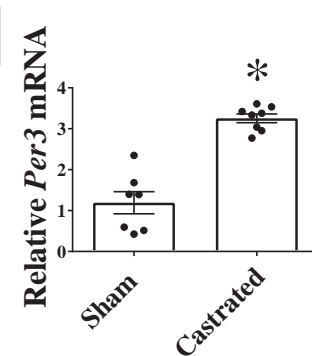
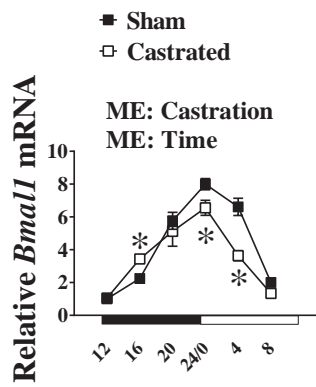
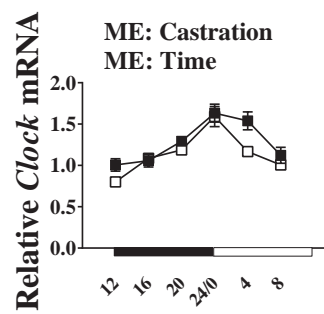
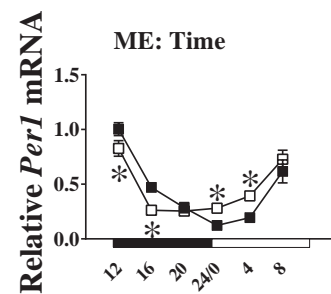
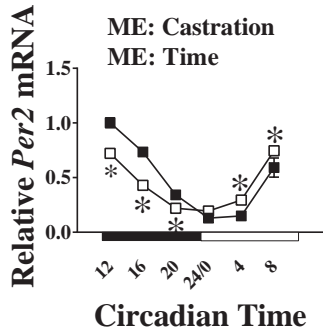
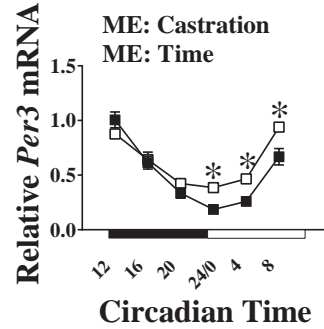
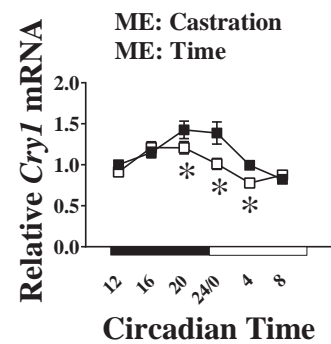
1196

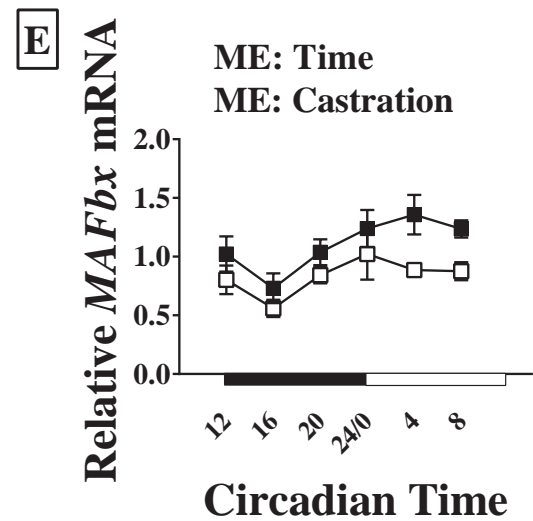
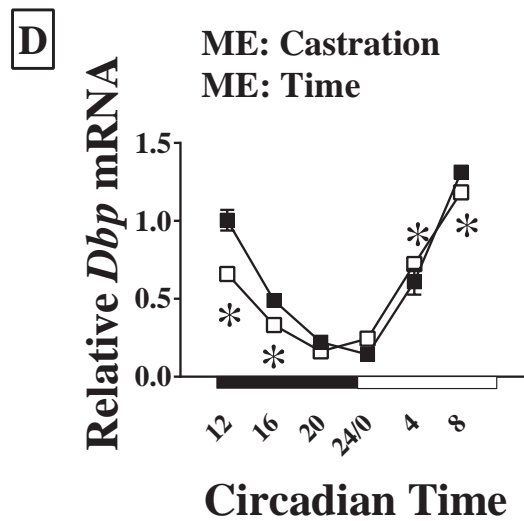
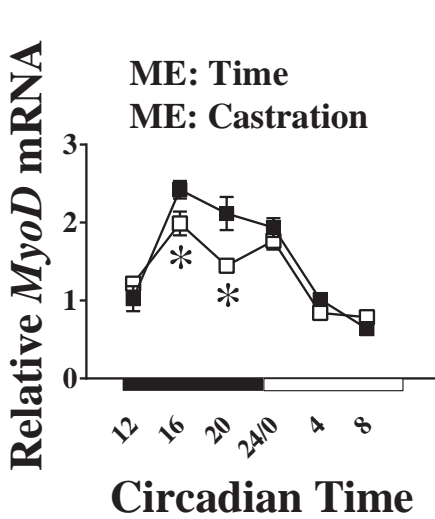
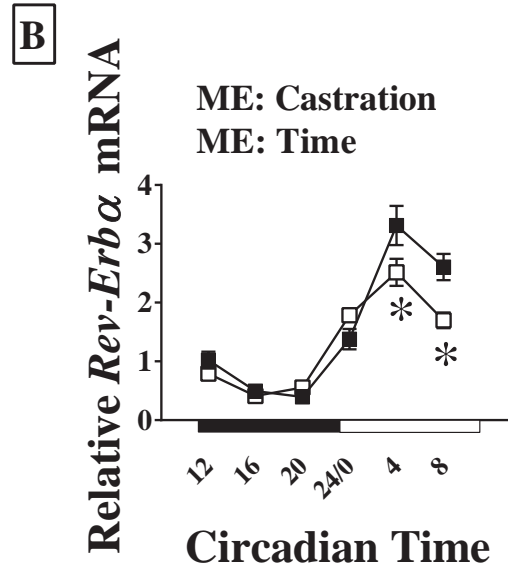
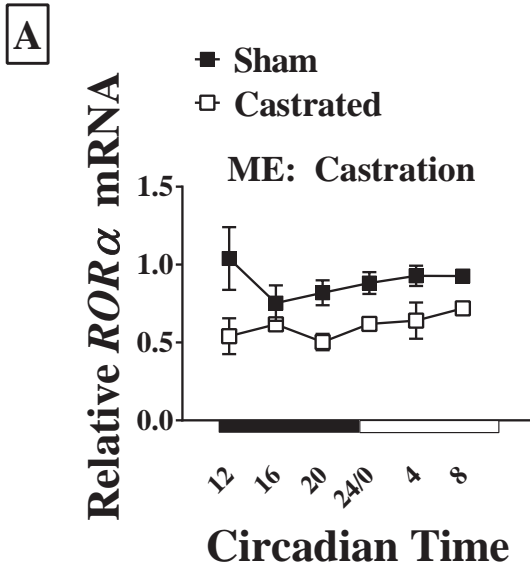
1197 Table 6: Body and Tissue Mass

	Sham (N = 18)	Castrated (N = 18)
Initial Body Weight (g)	26.7 ± 0.40	26.7 ± 0.39
Final Body Weight (g)	32.6 ± 0.61	29.4 ± 0.62*
Heart (mg)	139.29 ± 3.44	121.87 ± 2.54*
Spleen (mg)	64.56 ± 2.39	85.32 ± 1.39*
Epididymal Fat Pad (mg)	1035.64 ± 65.72	1129.28 ± 112.61
Seminal Vesicle (mg)	364.42 ± 14.16	11.03 ± 1.23*

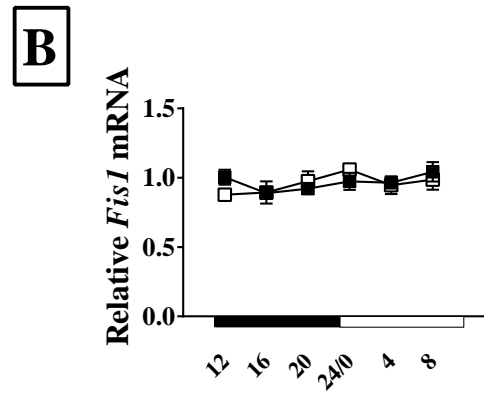
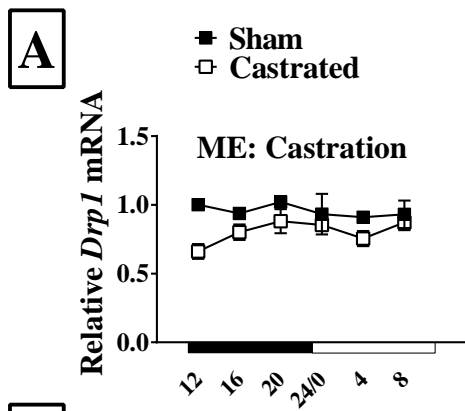
1198

1199

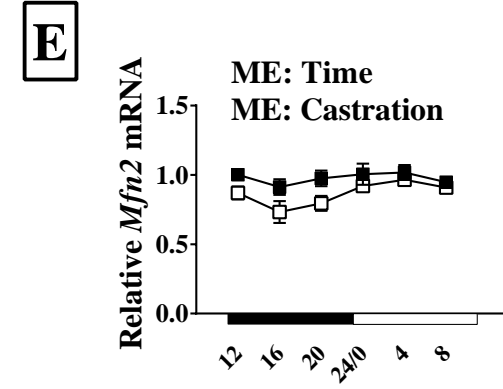
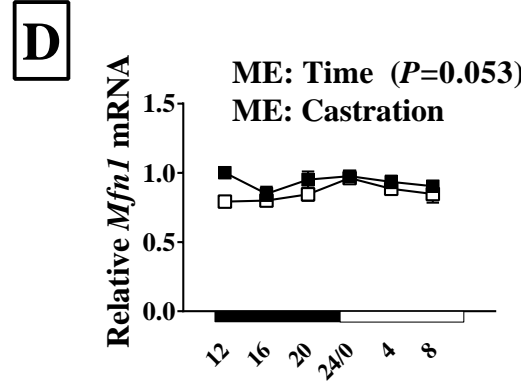
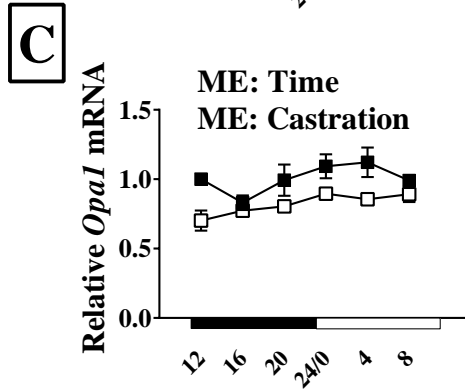
A**B****C****D****E****F****G****H****I****J**



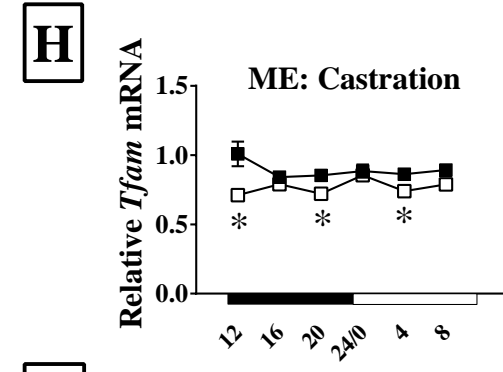
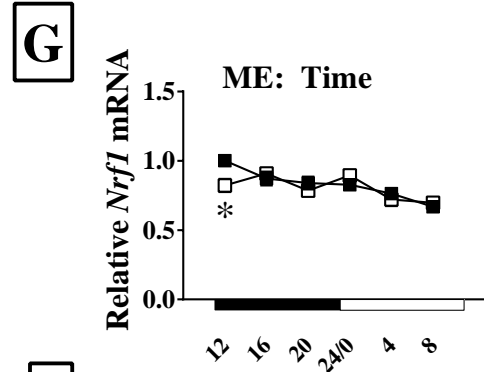
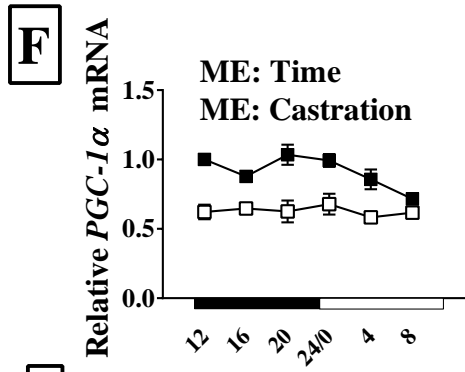
Fission



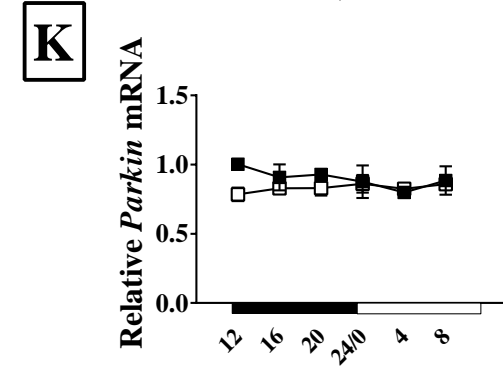
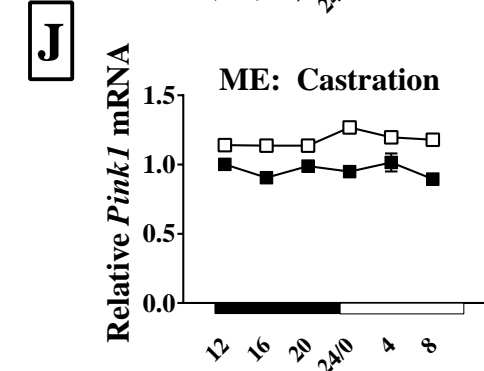
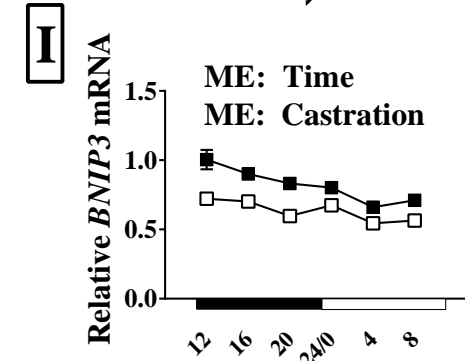
Fusion



Biogenesis



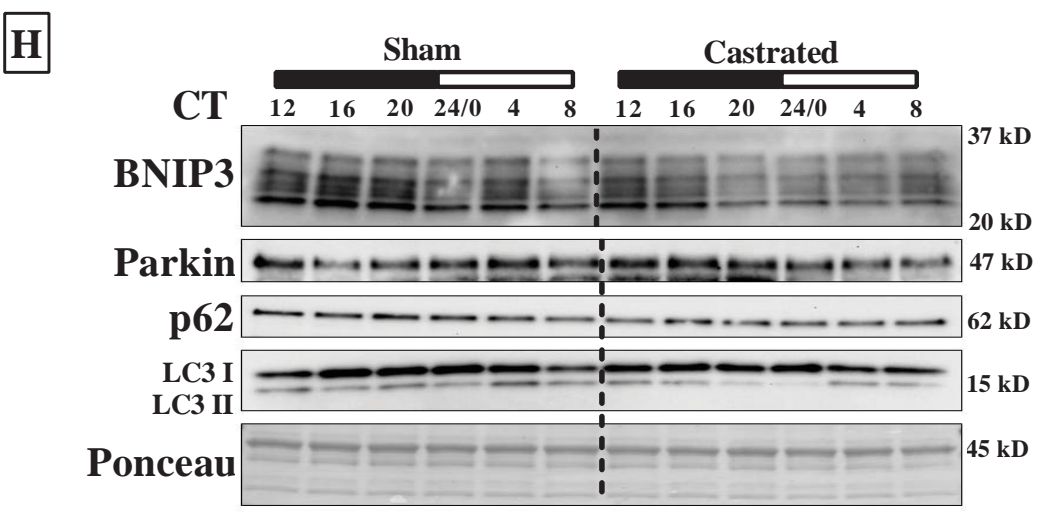
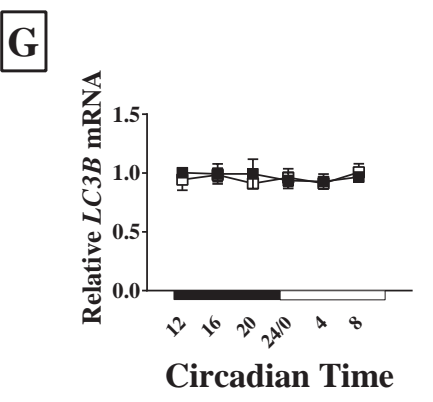
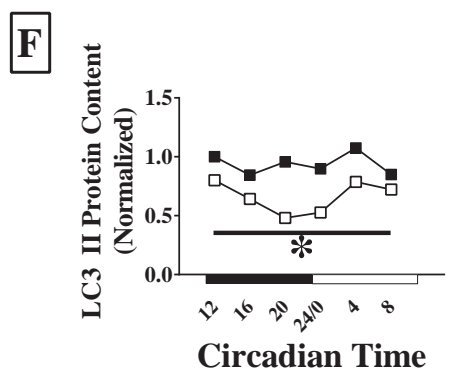
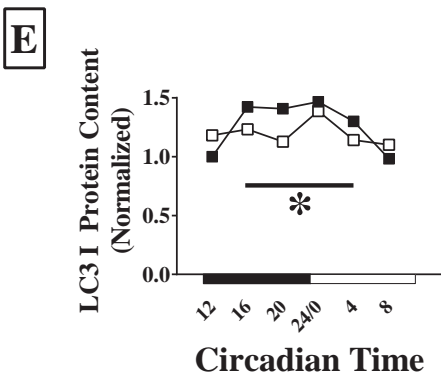
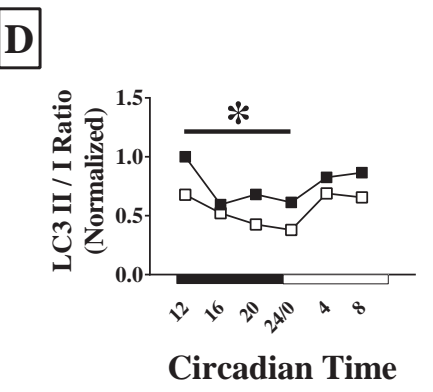
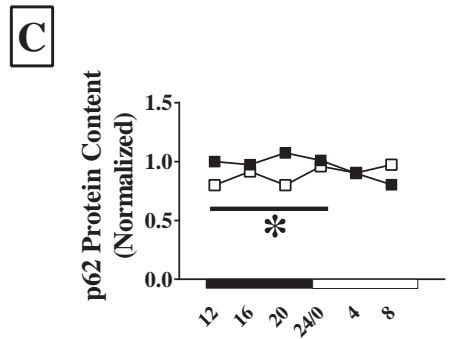
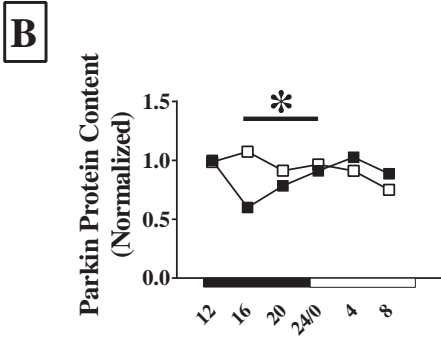
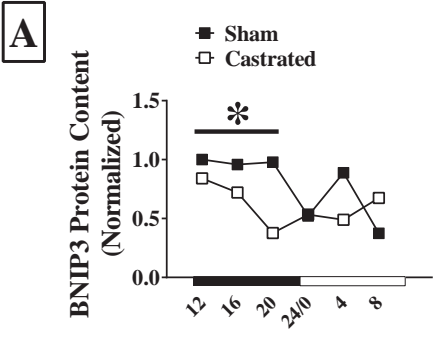
Mitophagy

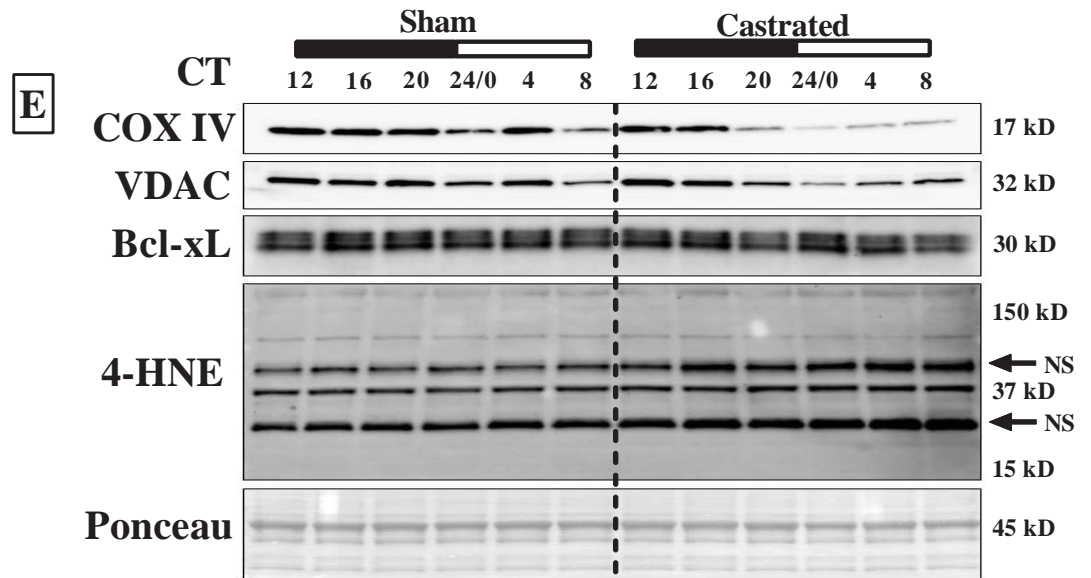
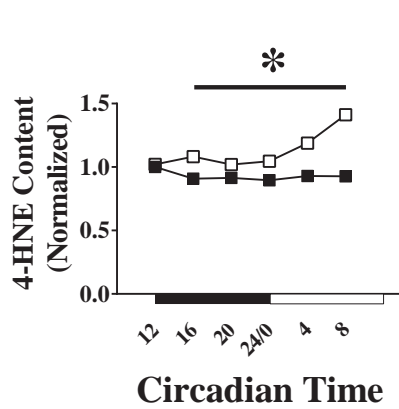
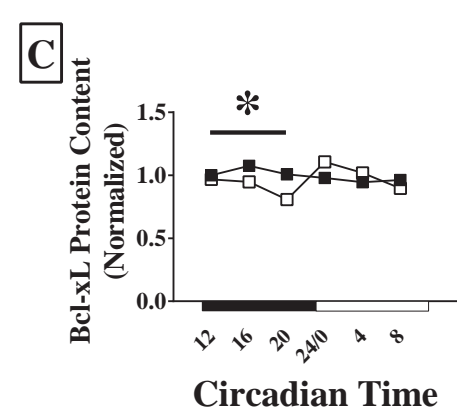
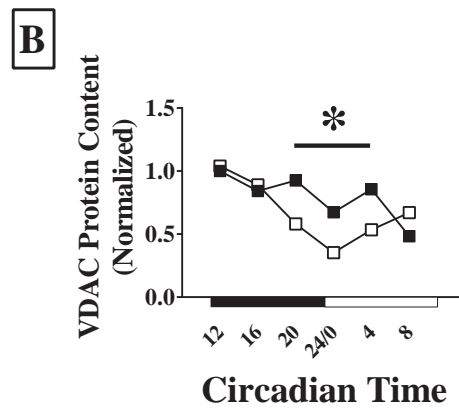
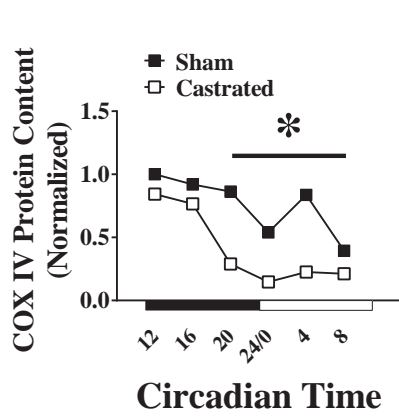


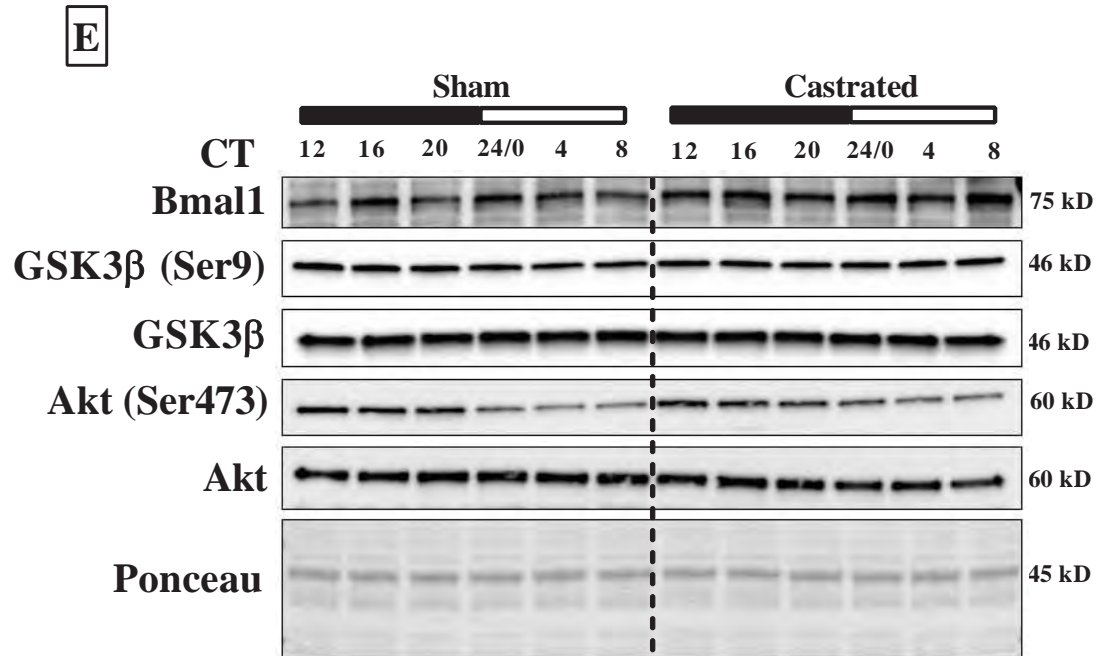
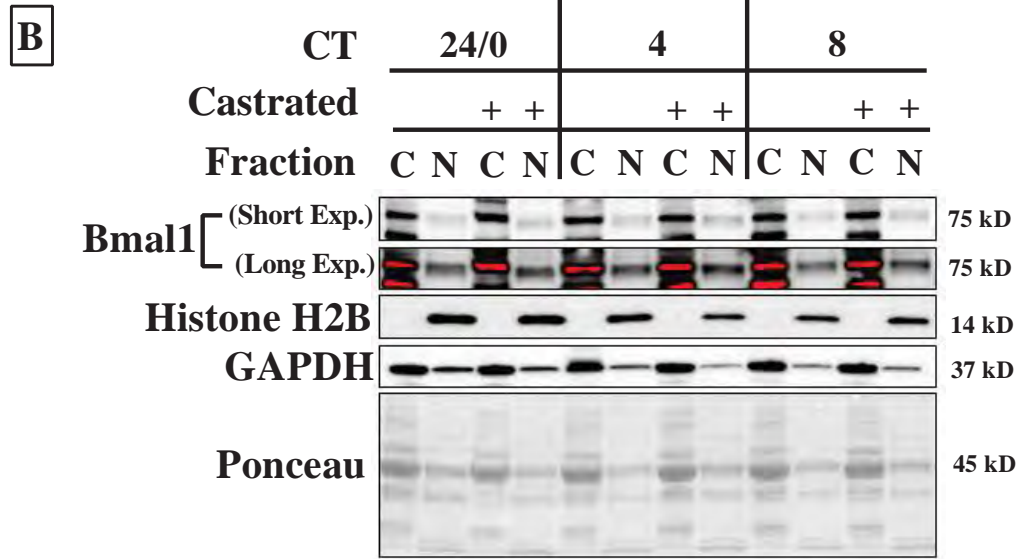
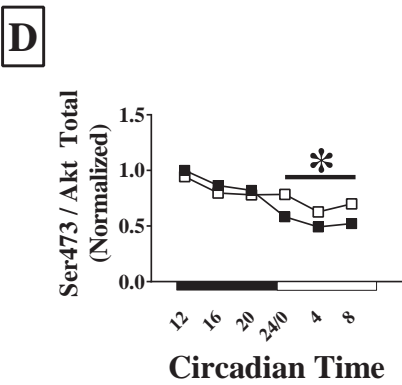
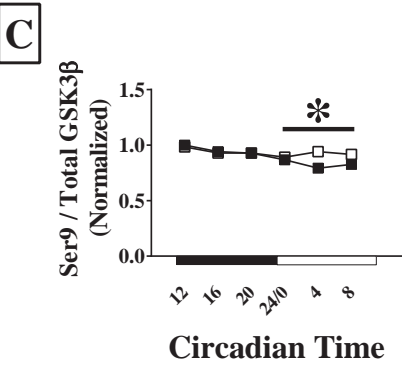
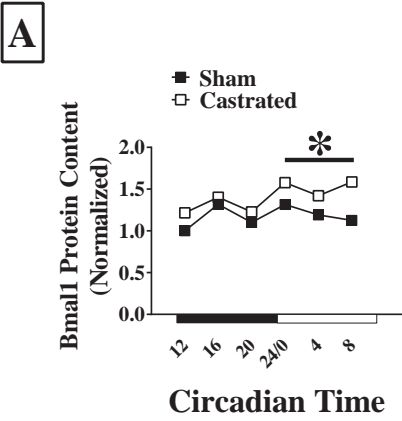
Circadian Time

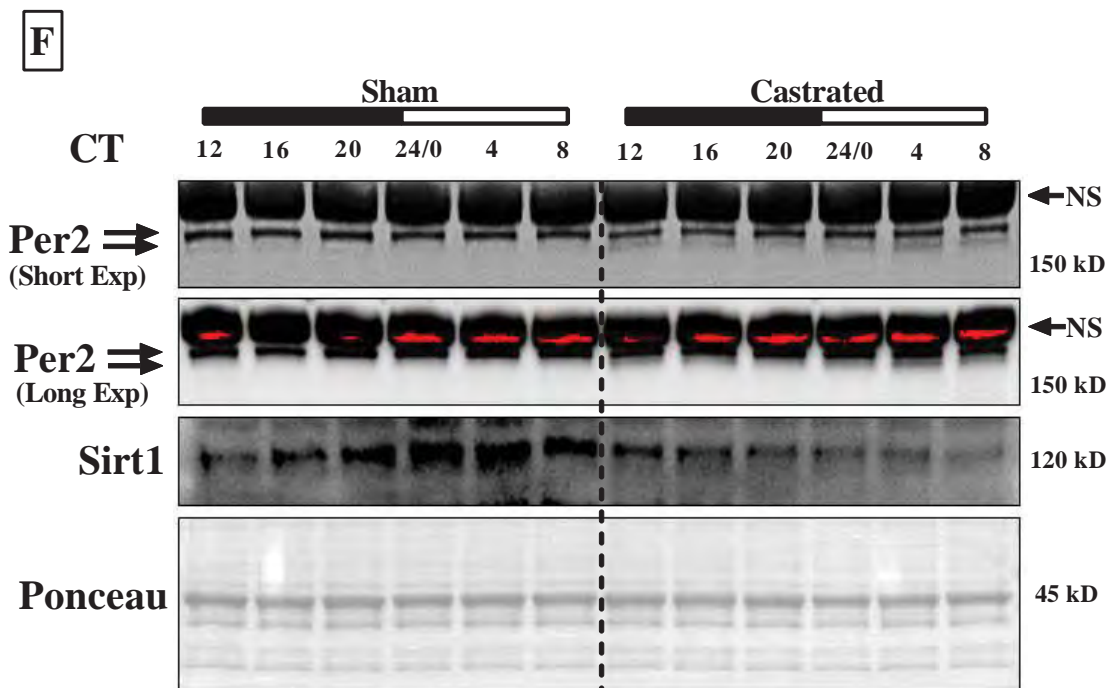
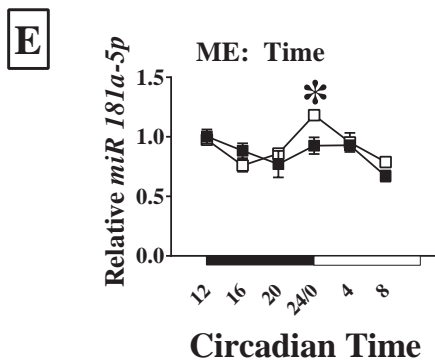
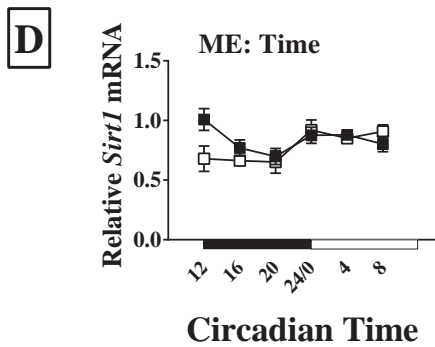
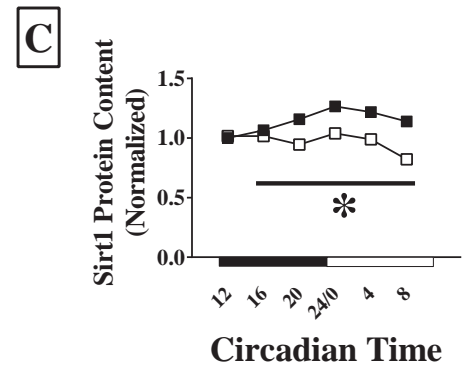
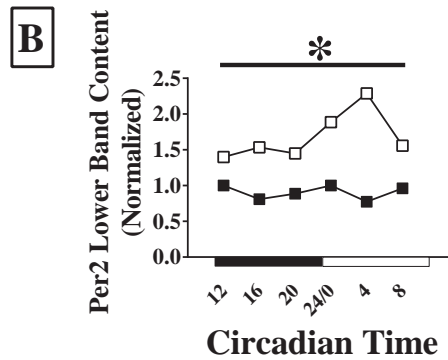
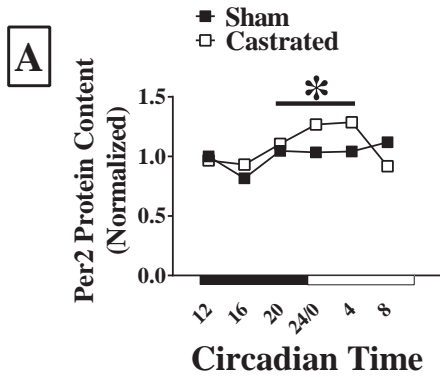
Circadian Time

Circadian Time

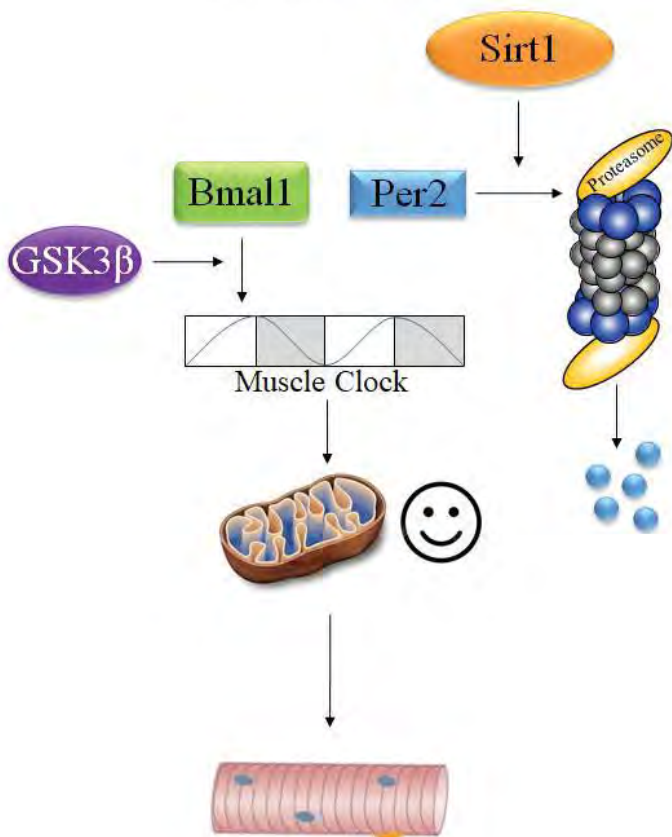








Androgen Sufficiency



Androgen Depletion

